

ISTANBUL TECHNICAL UNIVERSITY ★ INFORMATICS INSTITUTE

**A DUAL-BAND FREQUENCY SELECTIVE SURFACE DESIGN FOR
SATELLITE APPLICATIONS**



M.Sc. THESIS

Esma MUTLUER

Department of Communication Systems

Satellite Communication and Remote Sensing Programme

DECEMBER 2018

ISTANBUL TECHNICAL UNIVERSITY ★ INFORMATICS INSTITUTE

**A DUAL-BAND FREQUENCY SELECTIVE SURFACE DESIGN FOR
SATELLITE APPLICATIONS**



M.Sc. THESIS

**Esma MUTLUER
(705151007)**

Department of Communication Systems

Satellite Communication and Remote Sensing Programme

Thesis Advisor: Prof. Dr. Mesut KARTAL

DECEMBER 2018

İSTANBUL TEKNİK ÜNİVERSİTESİ ★ BİLİŞİM ENSTİTÜSÜ

**UYDU UYGULAMALARINDA KULLANILACAK ÇİFT BANTLI FREKANS
SEÇİCİ YÜZEY TASARIMI**

YÜKSEK LİSANS TEZİ

**Esmâ MUTLUER
(705151007)**

İletişim Sistemleri Anabilim Dalı

Uydu Haberleşmesi ve Uzaktan Algılama Programı

Tez Danışmanı: Prof. Dr. Mesut KARTAL

ARALIK 2018

Esma MUTLUER, a M.Sc. student of ITU Informatics Institute student ID **705151007**, successfully defended the **thesis/dissertation** entitled “**A DUAL-BAND FREQUENCY SELECTIVE SURFACE DESIGN FOR SATELLITE APPLICATIONS**”, which she prepared after fulfilling the requirements specified in the associated legislations, before the jury whose signatures are below.

Thesis Advisor : **Prof. Dr. Mesut KARTAL**
İstanbul Technical University



Jury Members : **Prof. Dr. Sedef KENT PINAR**
Istanbul Technical University



Doç. Dr. Hamid TORPİ
Yildiz Technical University



Date of Submission : 14 November 2018
Date of Defense : 14 December 2018





To my mother and father,



FOREWORD

I am grateful to my advisor Prof. Dr. Mesut Kartal who guided and supported me at every stage with his knowledge and experience in my thesis work.

I would like to thank Dr. Bora Döken for his support in both practical and theoretical subjects during my thesis study.

I would like to thank the ITU Research and Application Center for Satellite Communications and Remote Sensing (CSCRS) which provides financial support for the papers published in this thesis.

I would also like to thank Profen A.Ş for supporting us to use the necessary equipment for technical measurements.

I am always grateful to my family that I always feel their material and moral support.

December 2018

Esmâ MUTLUER
(Electrical Electronics Engineer)

TABLE OF CONTENTS

	<u>Page</u>
FOREWORD	ix
TABLE OF CONTENTS	xi
ABBREVIATIONS	xiii
LIST OF TABLES	xv
LIST OF FIGURES	xvii
SUMMARY	xxi
ÖZET	xxiii
1.INTRODUCTION	1
1.1 Purpose of Thesis	1
1.2 Literature Review	1
2.SATELLITE COMMUNICATION SYSTEMS	3
2.1 Frequency Bands	3
2.2 Antennas for Satellite Communication	4
2.2.1 Reflector antenna	4
2.2.1.1 Parabolic antenna	4
2.2.1.2 Cassegrain antenna.....	5
2.2.1.3 Offset parabolic antenna	5
2.2.2 Horn antenna	6
2.2.3 Helical antenna.....	6
3. FREQUENCY SELECTIVE SURFACE	9
3.1 Principle of Filters Theory	10
3.2 Factors That Govern the FSS Response	10
3.2.1 Shape of FSS elements.....	10
3.2.2 Effect of dielectrics substrate	11
3.2.3 Grating lobes	13
3.3 Analysis Methods of FSS	14
3.3.1 Finite difference time domain method	14
3.3.2 Finite element method.....	15
3.3.3 Methods of moment	15
3.3.5.1 Equivalent circuit method with FSS analysis	16
3.4 Application Areas of FSS.....	20
3.5 Use of FSS in Reflector Antennas.....	23
3.6 Manufacturing Methods of FSS	25
3.6.1 Implementation of FSS prints on FR4 layer	25
4. DESINGS	27
4.1 Design 1: A Novel Multi-Band FSS for Ka-Band Applications.....	28
4.2 Design 2: A Miniaturized Dual Ka/X Band Frequency Selective Surface	33
4.3 Design 3: A Dual- Band FSS Design for Satellite Applications.....	37
4.4 Comparison of Designs	45
5. FABRICATION AND MEASUREMENTS	47

6. CONCLUSIONS AND RECOMMENDATIONS	51
6.1 Improvement of Design Using Different Substrate Layers	52
REFERENCES	61
CURRICULUM VITAE	65
.....	65



ABBREVIATIONS

FSS	: Frequency Selective Surface
FSY	: Frekans Seçici Yüzey
TE	: Transverse Electric
TM	: Transverse Magnetic
ITU	: International Telecommunication Union
BSS	: Broadband Satellite Services
MSS	: Mobil Satellite Services
DBS	: Direct Broadcast Satellite Services
RCS	: Radar Cross Section
PEC	: Perfect Electrical Conductor
HFSS	: High Frequency Electromagnetic Field Simulation
S₁₁	: Reflection Coefficient
S₂₁	: Transmission Coefficient
ϵ_r	: Dielectric Constant
λ_r	: Dielectric Constant



LIST OF TABLES

	<u>Page</u>
Table 4.1 : Parameter values of first FSS	29
Table 4.2 : Parameter values of second FSS	33
Table 4.3 : Parameter values of last FSS.....	38
Table 4.4 : Comparasion of the proposed last FSS with the similar FSS	45
Table 4.5 : Comparasion of the all proposed FSSs with the similar FSS	45
Table 4.6 : S_{21} parameters in the proposed designs for TE mode	46
Table 4.7 : S_{21} parameters in the proposed designs for TM mode	46



LIST OF FIGURES

	<u>Page</u>
Figure 2. 1 : Frequency allocations for satellite communication services [30].	3
Figure 2. 2 : Principle of parabolic antenna [14].	4
Figure 2. 3 : Cassegrain Antenna [14].	5
Figure 2. 4 : Offset Parabol Antenna [14].	5
Figure 2. 5 : Horn Antenna types, pyramid horn antenna, conic horn antenna [14].	6
Figure 2. 6 : Relation of helix dimensions [14].	6
Figure 3. 1 : FSS types, transfer functions and EC Models,	9
Figure 3. 2 : (a) Low Transmittance (b) High Transmittance	10
Figure 3. 3 : Element type of FSS [1].	11
Figure 3. 4 : Effect of dielectric upon the resonant frequency [1].	12
Figure 3. 5 : FSS on the dielectric layer.	13
Figure 3. 6 : Grating Lobes (a) period $< \lambda$ (b) period $> \lambda$ [17]	13
Figure 3. 7 : Occurrence of unwanted propagations [1].	14
Figure 3. 8 : Periodic structure of parallel metal grids [24].	16
Figure 3. 9 : Square loop FSSs, parameters and equivalent circuit models [26]	18
Figure 3. 10 : Jerusalem Cross FSS parameters and equivalent circuit model [28]	19
Figure 3. 11 : A double-band reflective antenna [29].	21
Figure 3. 12 : A double band reflective antenna created using a flat reflector [1].	21
Figure 3. 13 : Hybrid antenna radome [29].	22
Figure 3. 14 : Use of FSSs as polarizers [1]	22
Figure 3. 15 : Reflector antenna structure with multiple working bands [39].	23
Figure 3. 16 : Reflector antenna design for Ka band signals with subreflector FSS	24
Figure 3. 17 : Reflector antenna design for Ka band and X band signals.	24
Figure 3. 18 : Reflector antenna design for Ka band and Ku band signals.	25
Figure 4. 1 : Geometry of FSS element	28
Figure 4. 2 : Boundary conditions for surface	29
Figure 4. 3 : Master and Slave boundary conditions	30
Figure 4. 4 : Floquet port for a unit cell in HFSS	31
Figure 4. 5 : S_{21} frequency for the first FSS geometry, TE polarization.	32
Figure 4. 6 : S_{21} frequency for the first FSS geometry, TM polarization.	32
Figure 4. 7 : Geometry of second FSS element	33
Figure 4. 8 : S_{21} frequency curves for the first design stages of second FSS	34
Figure 4. 9 : S_{21} frequency curves for the second design stages of second FSS	34
Figure 4. 10 : S_{21} frequency curves for the last design stages of second FSS	35
Figure 4. 11 : S_{21} frequency for the second FSS geometry, TE polarization.	35
Figure 4. 12 : S_{21} frequency for the second FSS geometry, TM polarization.	36
Figure 4. 13 : S_{11} frequency for the second FSS geometry.	36
Figure 4. 14 : Geometry of third FSS element	38
Figure 4. 15 : S_{21} frequency for the first design stages of the third FSS.	39
Figure 4. 16 : S_{21} frequency for the second design stages of the third FSS	40

Figure 4. 17 :	S_{21} frequency for the second design stages of the third FSS	40
Figure 4. 18 :	S_{21} frequency for the different value of the parameters including w1	41
Figure 4. 19 :	S_{21} frequency for the different value of the parameters.....	41
Figure 4. 20 :	EC model of FSS structure	42
Figure 4. 21 :	S_{21} frequency for the third FSS geometry, TE polarization	43
Figure 4. 22 :	S_{21} frequency for the third FSS geometry, TM polarization	43
Figure 4. 23 :	S_{11} frequency for the third FSS geometry	44
Figure 5. 1 :	FSS prototype	47
Figure 5. 2 :	A close view of the FSS prototype	47
Figure 5. 3 :	Measurement Equipment.....	48
Figure 5. 4 :	The location of the FSS in the test setup	48
Figure 5. 5 :	Measurement setup for Ka Band	49
Figure 5. 6 :	The location of the FSS in the test setup for Ku Band	49
Figure 5. 7 :	Measurement setup for Ku Band	50
Figure 6. 1 :	S_{21} frequency for the fourth FSS geometry,TE polarization	53
Figure 6. 2 :	S_{21} frequency for the fourth FSS geometry,TM polarization	53
Figure 6. 3 :	S_{21} frequency of the FSS designed using Rogers,TE polarization	54
Figure 6. 4 :	S_{21} frequency of the FSS designed using Rogers, TM polarization	54
Figure 6. 5 :	S_{21} frequency of the FSS using Taconik layer,TE polarization.....	55
Figure 6. 6 :	S_{21} frequency of the FSS using Taconik layer,TM polarization.....	55
Figure 6. 7 :	Modified Design	56
Figure 6. 8 :	S_{21} frequency of the new FSS using Taconik layer,TE polarization	56
Figure 6. 9 :	S_{21} frequency of the new FSS using Taconik layer,TM polarization...	57
Figure 6. 10 :	S_{21} frequency of the FSS using Rogers 3003 layer,TE polarization ..	57
Figure 6. 11 :	S_{21} frequency of the FSS using Rogers 3003 layer,TM polarization .	58
Figure 6. 12 :	S_{21} frequency of the FSS using Rogers 5880 layer,TE polarization ..	58
Figure 6. 13 :	S_{21} frequency of the FSS using Rogers 5880 layer,TM polarization .	59





A DUAL-BAND FREQUENCY SELECTIVE SURFACE DESIGN FOR SATELLITE APPLICATIONS

SUMMARY

Studies in the field of satellite communication have shown a great improvement from past to present. Firstly, satellites used in military field were developed and then commercial satellites were used. Satellite systems consist of three main components. These components can be classified as an earth station, ground terminal and satellite. In satellite communication systems, the antenna model which is widely preferred for communication between ground stations and satellites sufficiently is the reflector antennas. In the literature, there are several kinds of reflector antennas, but the reflector antenna types preferred in satellite applications grouped under three as “parabolic antennas”, “cassegrain antennas” and “offset parabolic antennas”. The most important advantages of using parabolic antennas are directing the radio wave with a narrow beam or allowing the waves to be received only at a certain angle. Reflector antennas are included of two parts; feeding and reflector. The feed part constitutes the electromagnetic wave source and the reflector part provides the antenna gain. Recent frequency selective surfaces in the reflector antenna designs, placed in two different ways which are between two feed points or behind a feed point. Frequency selective surfaces are structures that show transmission and reflection characteristics according to desired frequency. Frequency selective surfaces can be designed with multiple frequency characteristics, but also the frequency range of the designed frequency selective surfaces can be determined according to need. Because of these reasons, rapid developments in satellite technologies and the change of communication infrastructure over time increase the need for frequency selective surfaces. Moreover, studies on the design of these structures have been increased in order to reduce the number of reflectors in the satellites, to reduce the mass of the satellite and finally to reduce the cost. In this thesis, Ku band (14.1-16 GHz), Ka band (29.2-36.8 GHz) and X band (8-12 GHz) which are commonly used in satellite communication applications. In this thesis, three different frequency selective surfaces with suitable band stop characteristics are designed by selecting the target frequencies. Analysis, optimization and design studies are performed using the Ansoft HFSS program. Analysis results are evaluated by using parameters S11 (reflection coefficient) and S21 (transmission coefficient). In the first design, a frequency selective surface structure design with band stop characteristic is performed in more than one resonance frequency of the Ka band for simplicity. To create this structure with more than one resonance frequency, a new FSS structure is formed by combining two different hybrid geometry structures in a single layer. When the results of the first structure with band stop geometry were evaluated, it is observed that the transmission coefficient is at least -20 dB at two central resonance frequency (26.5 GHz and 43.5 GHz) up to 60 degree of incidence angle. In the second part of this study, a multi-band frequency selective surface design is performed in the Ka band (38.8 GHz-41.1 GHz) and X band (8 GHz-12 GHz). At

second design, we designed different geometries in different unit cells for Ka band and X band. Finally, these structures were combined in a single cell at a multi-frequency frequency selective surface.

Results show that the Ka band, one of the stop bands in the TE (transverse electric) and TM (transverse magnetic) modes, has shown an approximate of 2 GHz shift in both modes. The reason for this shift, is continuity of the geometry structure designed for the X band, in comparison with the miniaturized components of the structure designed for Ka band. The transmission coefficient of this structure is approximately -40 dB for X band and approximately -23 dB for Ka band. When the result is evaluated, the proposed second structure has a small size structure, two operating bands independently from each other and high selectivity. This designed frequency selective surface is proposed for use in a sub-reflector structure in reflector antennas.

In the final stage of this study, a dual band frequency selective surface design which can be used as a sub-reflector in the reflector antennas for satellite applications is performed in Ku (14.1 GHz-16 GHz) and Ka (29.2 GHz-36.8 GHz) band. In this design, a four-arm structure in the center is designed to reflect the Ku band signals. At the same time, in order to reflect the Ka band signal, two-legged structures are placed on the corners and four-legged structures are placed on each quadrant. To find the most ideal measurements of the geometric structures, the most preferred equivalent circuit model is used in the literature. In this FSS design, both S_{11} and S_{21} parameter values are observed. It is observed that for TE polarization the parameter S_{21} is at least -25 dB in the Ku band from 0 to 60 degrees, and a minimum in the Ka band is -20 dB. In TM mode, the transmission coefficient in both Ka and Ku bands is below -20 dB. This FSS structure has a small size and miniaturized structure considering the cell size. At the same time, it is understood that this structure has high selectivity when the parameters S_{11} and S_{21} are evaluated.

Totally three different designs are created in this thesis. All of these three designs are presented at international conferences.

UYDU UYGULAMALARINDA KULLANILACAK ÇİFT BANTLI FREKANS SEÇİCİ YÜZEY TASARIMI

ÖZET

Uydu haberleşmesi ile ilgili çalışmalar uzun yıllardır devam etmektedir. İlk olarak askeri alanda kullanılan uydular geliştirilmiş daha sonra ticari amaçlı uydular da kullanılmaya başlanmıştır. Uydu sistemleri üç ana birleşenden oluşmaktadır. Bu birleşenler bir yeryüzü istasyonu, yer terminali ve uydu olarak sınıflandırılabilir. Uydular yük (Payload) ve yol (Link) olmak üzere iki bileşenden oluşurlar. Yük bileşeninde antenler, alıcılar ve vericiler bulunurken, yol bileşeninde durum denetimi, sıcaklık denetimi, sıcaklık ve telemetri sistemleri (bir haberleşme ağı ile sistemlerin uzaktan kablosuz izlenmesi) bulunur. Uydu haberleşme sistemlerinde, yer istasyonlarının uydu ile yeterli güçte haberleşebilmesi için yaygın olarak tercih edilen anten modeli reflectör antenlerdir. Uydu uygulamalarında tercih edilen reflector anten çeşitlerini “parabolik antenler”, “cassegrain antenler” ve “offset parabolic antenler” olmak üzere üç grup altında toplayabiliriz. Parabolik antenlerin kullanılmasının en önemli avantajları radyo dalgasının dar bir ışınla yönlendirmek ya da sadece belli bir yönden dalgaların alınmasını sağlamaktır. Diğer bir avantajı ise dar bir ışın demeti genişliği üreterek daha yüksek kazanç sağlamalarıdır.

Reflektör antenler besleme ve reflektör olmak üzere iki kısımdan oluşur. Besleme kısmı elektromanyetik dalga kaynağını oluştururken, reflektör kısmı antenin kazancını sağlamaktadır. Son zamanlarda, reflektör anten tasarımlarında iki besleme noktasının arasına yada bir besleme noktasının arkasına yerleştirilecek şekilde frekans seçici yüzeyler kullanılmaya başlanmıştır.

Frekans seçici yüzeyler frekansa göre değişebilen iletim ve yansıma özellikleri gösteren yapılardır. Bu yapılar bir dielektrik yüzeye yerleştirilerek periodik iletken yama veya açıklıklar şeklinde tasarlanır. Frekans seçici yüzeyler anten ve mikrodalga alanında bir çok uygulamada kullanılmaktadır fakat uydu uygulamalarında kullanımı son bir kaç yıla dayanmaktadır. Uydularda bulunan reflector sayısını azaltmak, uydunun ağırlığını azaltabilmek ve son olarak maliyeti düşürebilmek için bu yapıların tasarımları üzerine çalışmalar başlamıştır. Frekans seçici yüzeyler birden fazla frekans karakteristiğine sahip olarak tasarlanabilir, aynı zamanda tasarlanan frekans seçici yüzeylerin frekans aralığı ihtiyaca uygun olarak belirlenebilir. Bu sebeplerden dolayı uydu teknolojilerindeki hızlı gelişmeler ve haberleşme alt yapısının zamanla değişmesi frekans seçici yüzeylere olan ihtiyacı arttırmaktadır.

Uydu haberleşme uygulamalarında Ka bant (26.5- 40 GHz), Ku bant (12- 18 GHz) ve X bant (8-12 GHz) frekans bantları yaygın olarak kullanılmaktadır. Bu tez çalışmasında Ku bandında 14.1-16 GHz , Ka bandında 29.2-36.8 GHz ve X bandında 8- 12 GHz frekans aralıkları kullanılmak üzere seçilmiştir. Tez çalışması kapsamında amaca uygun bant durdurma karakteristiğine sahip bir yüzey malzemesi belirlenen hedef frekanslar seçilerek tasarlanmıştır.

Bu tez çalışmasında, ilk olarak uydu uygulamalarında kullanılan anten yapıları incelenmiş, frekans seçici yüzey geometrileri araştırılmıştır. Tasarım aşamasında literatürde de en çok kullanılan yöntem olan eşdeğer devre yönteminden yararlanılmıştır. Analiz, optimizasyon ve tasarım çalışmaları Ansoft HFSS programı kullanılarak gerçekleştirilmiştir.

Analiz sonuçları S_{11} (yansıtma katsayısı) ve S_{21} (iletim katsayısı) parametreleri kullanılarak değerlendirilmiştir. Bu çalışma kapsamında hedeflenen frekans bantları durdurulduğunda yüzey malzemesinin S_{11} parametresinin maksimum -3 dB , S_{21} parametresinin ise minimum -10 dB olması hedeflenmiştir.

Bu tez çalışmasında üç farklı tasarım üzerinde çalışılmıştır. İlk olarak basitlik açısından sadece Ka bandında birden fazla rezonans bölgesinde bant durdurucu karakteristiğe sahip bir frekans seçici yüzey yapısı tasarımı amaçlanmıştır. Bu iki rezonanslı yapıyı oluşturmak için, hibrit geometriden oluşan iki farklı yapının tek bir katmanda birleşmesi ile literatürden farklı yeni bir FSY yapısı oluşturulmuştur. Önerilen bu frekans seçici yüzey, Ka bantta hedef olarak seçilen frekans aralığında (25.5-27.3 GHz ve 41.8-45.1 GHz) ve 60 dereceye kadarki geliş açılarında frekans durdurma özelliğine sahiptir. Bant durdurma geometrisine sahip bu yapının sonuçları değerlendirildiğinde seçilen iki merkez rezonans değerlerinde (26.5 GHz and 43.5 GHz) iletim katsayısının minimum -20 dB olduğu gözlemlenmiştir.

Tez çalışmasının ikinci adımında birden fazla frekans bandında bant durdurma özelliğine sahip frekans seçici yüzey tasarımlarının gerçekleştirilmesi hedeflenmiştir. Çok bantlı FSY tasarımlarının ilkinde Ka bandında 38.8 GHz- 41.1 GHz ve X bandında 8 GHz- 12 GHz belirtilen frekans bölgelerinde çalışan bir frekans seçici yüzey tasarımı gerçekleştirilmiştir. Seçilen her iki bant (Ka ve X) aralığı için o bantlara özel geometriler tasarlanmıştır. Simülasyon sonuçları incelendiğinde TE (enine elektrik) ve TM (enine manyetik) modlarında geliş açısına bağlı olarak durdurma bantlarından biri olan Ka bandında her iki modda da yaklaşık olarak 2 GHz kayma meydana geldiği gözlemlenmiştir. TE modunda 0 derece geliş açısında istenilen frekans aralıklarında (X bandı için 8-12 GHz, Ka bandı için 38-41 GHz) tasarlanan FSY yapısı bant durdurucu özelliğe sahipken, aynı modda 15 ve 45 derecede Ka bandında 40.8 GHz – 43.6 GHz aralığında ve 34 GHz- 35.6 GHz aralığında bant durdurucu özellik göstermektedir. TM modunda ise 0 derece geliş açısında istenilen frekans aralıkları olan 8 GHz-12 GHz ve 38 GHz- 41 GHz değerlerinde bant durdurucu özellik gösterirken, 15 derece geliş açısında yaklaşık olarak 1 GHz kayarak 37.8 GHz – 38.9 GHz değerlerinde durdurma özelliği göstermektedir. TM modunda 40 derece geliş açısında ise yine yaklaşık olarak 1 GHz kayma gözlenerek durdurma bantı frekansları 36.4 GHz- 37.2 GHz aralığında gözlemlenmiştir. Bunun nedeni X bandı için tasarlanan geometri yapısının süreklilik gösterirken, Ka bandı için tasarlanan geometrik yapıların minyatürüne şekilde olması ve süreklilik göstermemesidir. Önerilen bu yapı küçük hücre boyutuna, birbirinden bağımsız çalışan iki çalışma bandına ve yüksek seçiciliğe sahiptir. Tasarlanan bu yapıda iletim katsayısı X bant için yaklaşık olarak -40 dB , Ka bant için iletim katsayısı ise yaklaşık olarak -23 dB' dir. Tasarlanan bu frekans seçici yüzey reflektör antenlerde bir alt reflektör yapısı halinde kullanımına uygun olarak tasarlanmıştır.

Tez çalışmasının son adımında uydu uygulamalarında reflektör antenlerde alt reflektör olarak çalışabilen, Ku (14.1 GHz-16 GHz) ve Ka (29.2 GHz-36.8 GHz) bandında bant durdurma özelliği gösteren çift bantlı bir frekans seçici yüzey gerçekleştirilmiştir. Bu tasarımda Ku bant sinyallerini yansıtmak için merkeze

yerleştirilmiş dört kollu bir yapı tasarlanmıştır, aynı zamanda Ka bant sinyallerini de yansıtılabilmek için köşelere yerleştirilmiş iki ayaklı yapılar ve her bir kadrana yerleştirilmiş dört ayaklı yapılar tasarlanmıştır.

Önerilen bu yapının hücre boyutu en büyük dalga boyu için " $0.2\lambda \times 0.2\lambda$ " 'dir. Tasarılan geometrik yapıların en ideal ölçülerini bulabilmek için literatürde en çok tercih edilen eşdeğer devre modelinden yararlanılmıştır. Bu FSY tasarımında simülasyon sonuçlarında hem S_{11} hem de S_{21} parametre değerleri gözlemlenmiştir. S_{21} parametresinin 0 dereceden 60 derece gelme açısına kadar TE polarizasyonunda Ku bandında minimum -25 dB'in altında, Ka bandında ise minimum -20 dB olduğu gözlemlenmiştir. TM modunda ise hem Ka hem de Ku bandında iletim katsayısı -20 dB' in altındadır. S_{11} yansıma katsayısı istenilen frekans aralıklarında (Ka bant için 29.2 GHz-36.8 GHz, Ku bant için 14.1 GHz-16 GHz) Ka bandında -0.4 dB, Ku bandında maksimum -0.6 dB olduğu gözlemlenmiştir. Bu sonuçlar değerlendirildiğinde FSY yapısının absorber olarak değil bant durdurucu olarak çalıştığı açıkça gözlemlenmiştir. Ayrıca, iletim katsayısının TE polarizasyonunda elektromanyetik dalganın geliş açısının artması ile arttığı ve TM polarizasyonunda ise elektromanyetik dalganın geliş açısının artması ile azaldığı gözlemlenmiştir. Bu çalışmada , 35 GHz bandı incelendiğinde 15 GHz bandına göre kararlılığın daha az olduğu görülmektedir. Bunun nedeni ise, 15 GHz için kullanılan geometri yapısı 35 GHz için kullanılan geometri yapılarından boyut olarak daha büyüktür. Bu durum elektromanyetik dalganın geliş açısının geometrik yapıdan etkilendiğini açık bir şekilde göstermektedir. Tasarlanan bu FSY yapıda hücre boyutuna bakıldığında hem küçük boyutta ve minyatürize yapılara sahip olduğu hem de S_{11} ve S_{21} parametreleri değerlendirildiğinde bu yapının yüksek seçiciliğe sahip olduğu anlaşılmaktadır. Aynı zamanda TE ve TM modlarında 60 derece geliş açısına kadar kararlı bir yapı göstermektedir.

Birden fazla durdurma bandına sahip FSY tasarımlarında istenilen frekans bantlarında bant durdurma özelliği sağlayabilmek için farklı geometriler kullanılır. Bu geometriler birbirine çok yakın olduğu durumlarda ya da çok fazla minyatürize yapılar kullanıldığında farklı frekans bantlarında girişimler meydana gelmektedir. Tez çalışması kapsamında tasarlanan üç yapıda da bu sorunla karşılaşmıştır. Literatürde bu problemi çözebilmek için çok katmanlı FSY'ler kullanılmış ve her bir katmanda farklı frekans bantları için tasarımlar gerçekleştirilmiştir. Bu durum tasarımın zorlaşmasına neden olmaktadır. Bu tez çalışması kapsamında çözüm olarak daha minyatürize yapılar kullanılmaya çalışılmış, farklı frekans bantlarına karşılık olarak kullanılan geometriler arası mesafe arttırılmıştır ve çok katmanlı yapılar yerine tek katmanlı yapı kullanılmıştır. Böylece tasarımın kolaylaştırılması amaçlanmıştır. Bu çalışmalar ile birlikte optimum parametreleri bulmak için eşdeğer devre modelinden yararlanılmıştır.

Tez süresince üç adet birbirinden farklı tasarımlar meydana getirilmiştir. Bu tasarımların üçü de uluslararası konferanslarda sunulmuştur.





1.INTRODUCTION

1.1 Purpose of Thesis

Recently, there is a growing need to the multi-band reflector antenna systems for satellite applications. FSSs are employed in the multiband reflector antenna systems as a sub-reflector in order to reduce the number of reflectors, minimize the mass and reduce the cost of systems. FSSs simply separate the feed antenna signals of the antenna system by the reflection and transmission frequency responses. In the thesis study, it is aimed to design a frequency selective surface which has a good transmission characteristic, at the same time other frequency values stops in accordance with the Ka/Ku/X band frequency values.

1.2 Literature Review

FSS studies were initiated by Marconi and Franklin in 1919 [1]. Over time, the use of these structures has increased in many applications such as satellite communication [2], artificial magnetic conductor design, high selective spatial filter [3], microwave polarization converter, dichroic reflector surfaces, and subreflector design for large aperture antennas, airborne radomes [4]. In recently year, several FSS structures used in satellite applications have been proposed. A two layer of FSS with reflection features utilizing the X band and the Ka band was designed in [3]. In the X-/Military Ka band, a single aperture reflectarray using cascade configuration for each band to reduce the coupling between the elements of these two bands are presented in [5]. FSS which transmits Ka-band signals (17.3–20.2 GHz) while reflects Ku-band signals (11.7–12.75 GHz) and conserve circular polarization in each of these bands is presented in [6]. A single layer FSS that operates for an oblique angle of incidence in X(9.4GHz), Ku (14.5 GHz) and Ka (35 GHz) bands for dual polarization is presented in [7]. A novel dual pass-band FSS geometry operating at Ka band is designed in [8]. An ultrathin and polarization-insensitive FSS having a 3 dB bandwidth from 33 GHz and 37.5 GHz in Ka band is designed in [9]. In addition, this structure accomplishes

the necessary conditions for radome applications with a flat passband, sharp roll-off and stable polarization frequency response. Low-profile second or third-order band-pass FSS design utilizing nonresonant elements is presented in [10] as a new technique. Proposed second order band-pass microwave filter topology is improved in [11] with a FSS design having two passbands at X and Ka band. With the technique presented in [11], it is possible to design and optimize a dual-band FSS having independent frequency bands from each other. A double layer FSS structure having a first-order band-pass response is presented in [12]. This frequency behavior is achieved by using cascaded spatial lumped elements.



2.SATELLITE COMMUNICATION SYSTEMS

2.1 Frequency Bands

ITU (The International Telecommunication Union) has defined many different services for use in satellite systems. The major ones are these services fixed satellite services, broadband services (BSS) and mobile satellite service (MSS).

All radio communication services operated include fixed satellite services such as INTELSAT, EUTELSAT, and PANAMSAT etc. Broadband services include the area of direct broadcasting satellites (DBS). This consists of much smaller earth stations on domestic premises together with fixed earth stations providing the uplink feeder to the satellite [13]. Mobile satellite services operate in the maritime Mobil service, aeronautical mobile service and land mobile service. The above-mentioned services consist of earth terminals located in mobile phones and fixed base stations. International agreements are made for the spectrum allocation to be used in the services. Different satellite operators used different spectrum. Therefore, coordination is ensured to prevent excessive interference. The spectrum ranges used for satellite communication are shown in Figure 2.1.

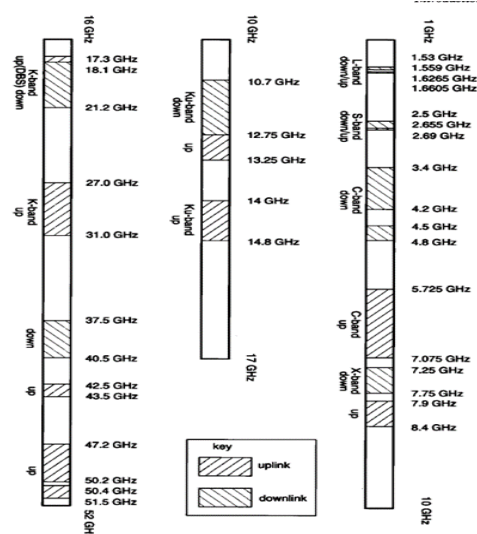


Figure 2. 1 : Frequency allocations for satellite communication services [30].

2.2 Antennas for Satellite Communication

Antennas are structures that provide communication between ground stations and various satellite subsystems. These structures receive the uplink signal and transmit to downlink signals. Moreover, gain values determine the amount of power received directly. Some of the antenna types used in satellite applications are reflector antenna, horn antenna, helical antenna and phased antenna.

2.2.1 Reflector antenna

Reflector antennas are used both in satellite communication and broadcast satellite receive antennas. Reflector antennas convert the spreading spherical wave into a plane wave, thus achieving high gain and low side lobes. Reflector antennas can be divided into four groups in itself [14];

- Parabolic antenna
- Cassegrain antenna
- Offset parabolic antenna
- Offset Cassegrain antenna

2.2.1.1 Parabolic antenna

Parabolic antennas are used in many applications related to radio, television and data communication. As shown in Figure 2.2, parabolic antennas consist of a combination of the parabolic reflection surface and the feed part in a centered position.

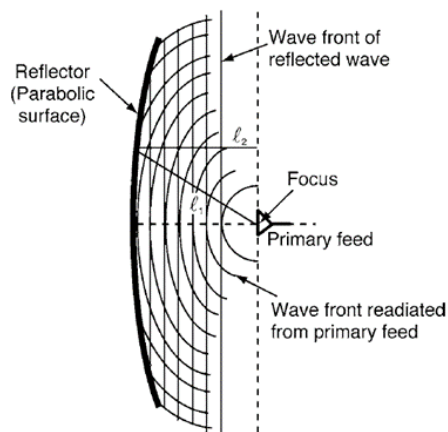


Figure 2. 2 : Principle of parabolic antenna [14].

For this structure, the feed point is placed in the reflector focus of the antenna, so the gain is low. The Cassegrain antenna, which is the advanced model of this structure, will be mentioned in the next section.

2.2.1.2 Cassegrain antenna

This antenna consists of a parabolic surface, a main reflector, and a sub-reflector. The main reflector is used as a transducer between the spherical waves and the plane waves, while the lower reflector works like a spherical waveform converter.

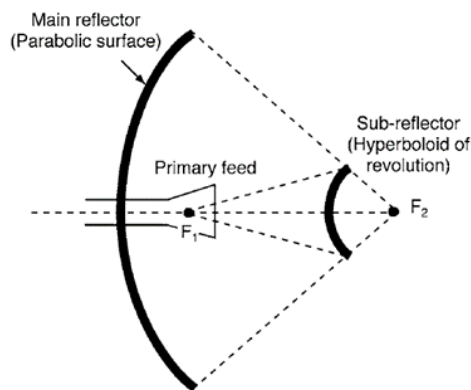


Figure 2. 3 : Cassegrain Antenna [14].

2.2.1.3 Offset parabolic antenna

While sub-reflectors located on the Cassegrain antenna are placed in front of the main reflector, sub-reflector and feed located on offset parabolic antenna sets outside of the aperture. Therefore, the gain is increased, at the same time the effect of side lobes is reduced. The structure of this antenna is shown in Figure 2.4.

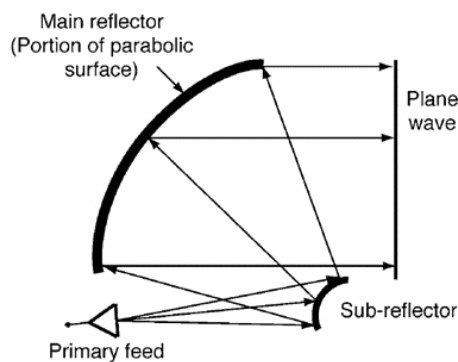


Figure 2. 4 : Offset Parabolic Antenna [14].

2.2.2 Horn antenna

Horn antennas were first introduced in 1959 by the national aviation and space agency for passive communication satellite project. The most important features of the horn antenna are the fact that the side lobes are very small, broadband and has calculable aperture efficiency. The horn antennas have two types, as shown in Figure 2.5.

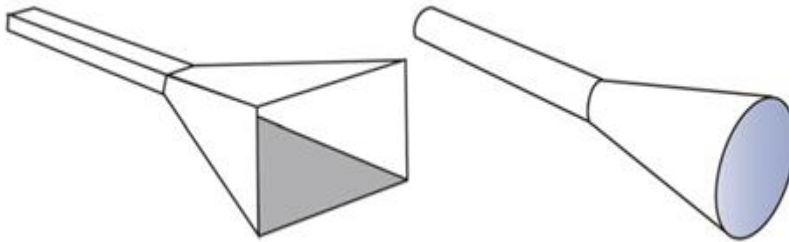


Figure 2. 5 : Horn Antenna types, pyramid horn antenna, conic horn antenna [14].

The horn antenna is generally used as a reference antenna to measure the gain of the various antennas. The reason is that horn antennas are generally equal to the theoretical gain of the measured gain.

2.2.3 Helical antenna

Helical antenna is a type of antenna consisting of helical, loop and wires. The radiation is smaller than the wavelength of the spiral when the maximum for the helical axis. As it changes to the helical geometry, the radiation pattern changes to elliptical, planar or circularly polarized [15].

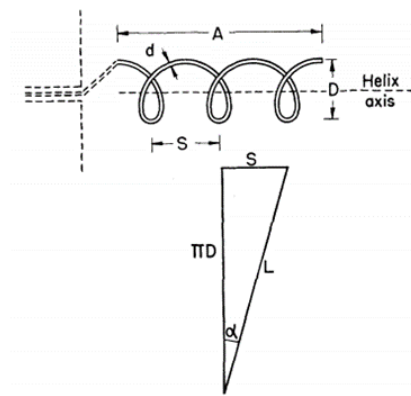


Figure 2. 6 : Relation of helix dimensions [14].

Where, **D** is diameter of helix (center to center), **S** is spacing between turns, **α** is pitch angle, **L** is length of one turn, **n** is number of turns, **A** is axial length and **d** is diameters of helix conductor.





3. FREQUENCY SELECTIVE SURFACE

The frequency selective surface is periodic conductive or slot array structure placed on dielectric surfaces. These structures, which are usually supported by a sublayer or embedded in this layer, turn into a resonance periodic structure by providing selectivity in frequency, polarization and incidence angle. Therefore, it can reflect or transmit electromagnetic waves according to desired frequency values [1, 2]. These filter behaviors are as shown in Figure 3.1.

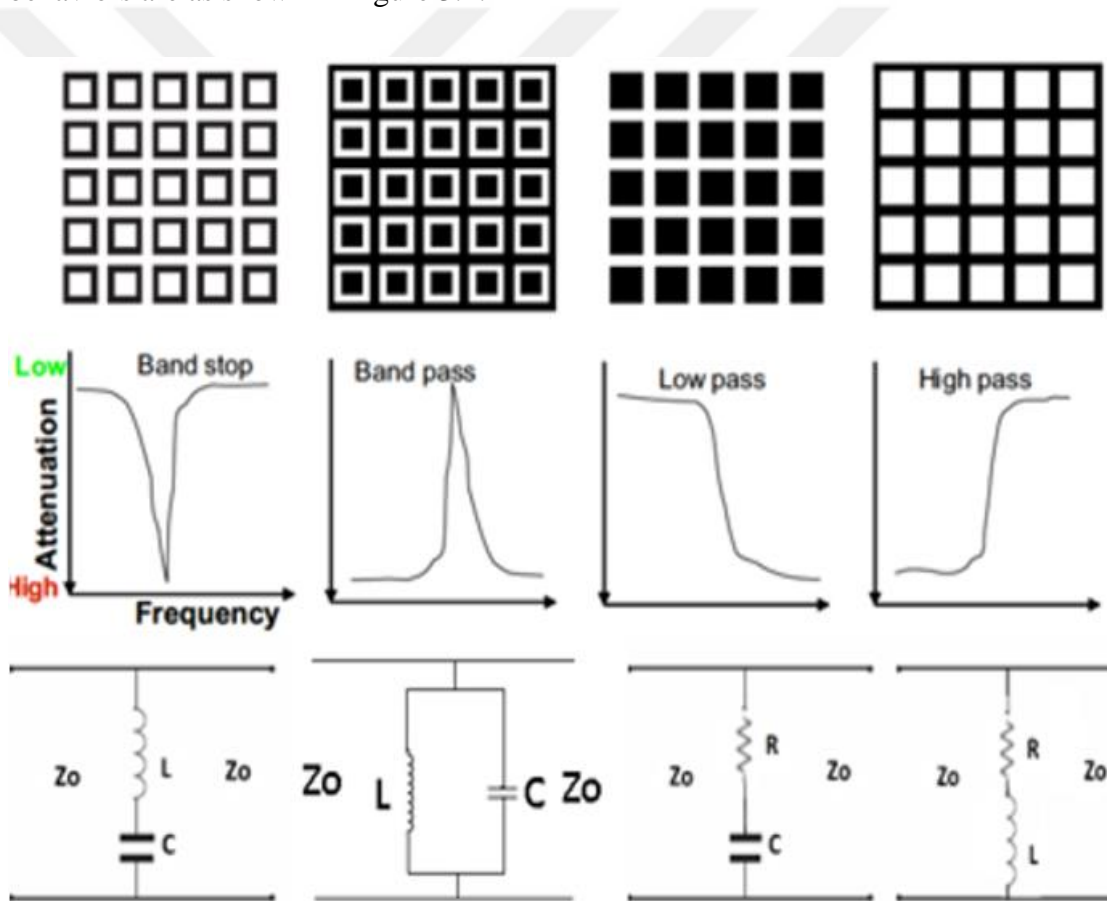


Figure 3. 1 : FSS types,transfer functions and EC Models,

The reflection and transmission characteristics of these selective surfaces rely on the polarization, angle of the incident wave, the frequency, and the absorption and re-radiation efficiency of the conductive and dielectric materials used.

3.1 Principle of Filters Theory

In order to understand the FSS structures, the working principle of the filters will be mentioned first. When an incident plane wave hits the filter, it causes the electrons in the metal to be released. Most of the incident energy is absorbed by these electrons, thus re-radiation occurs in the starting area. This causes the energy transmitted to the filter to be reduced. Therefore, the electrons will re-radiate toward the left and cause the reflected wave amplitude to be high [16]. On the other hand, transmittance is high when only a small part of the incidence power is absorbed. Consequently, the electrons in the metal absorb some wavelengths higher than others and re-radiate some wavelengths. The principles mentioned above are given in Figure 3.2.

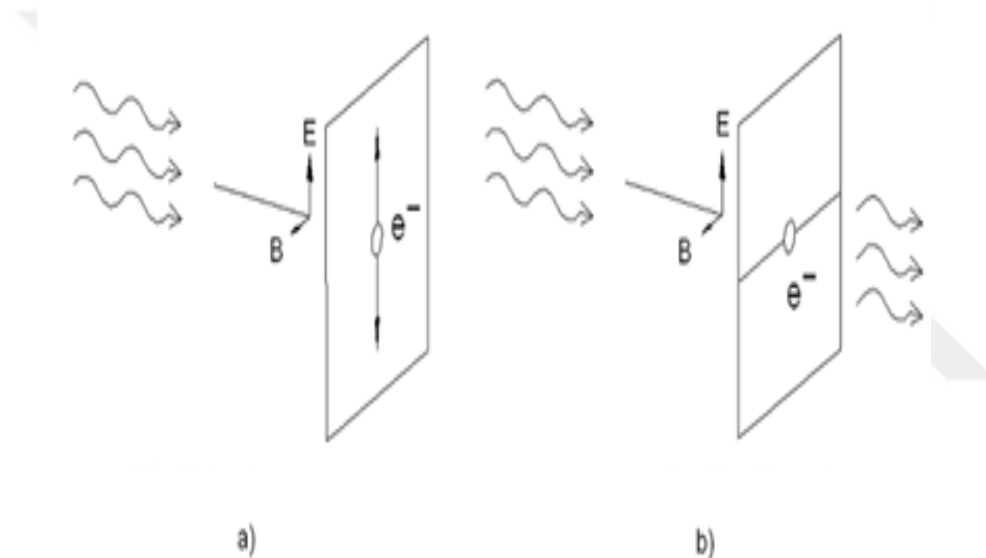


Figure 3. 2 : (a) Low Transmittance (b)High Transmittance

3.2 Factors That Govern the FSS Response

3.2.1 Shape of FSS elements

According to Munk's book, FSS element structures can be explained in 4 groups; the first group is connected to the center, or the N poles such as a simple flat element, a triplet element; anchor elements; Jerusalem cross; and square spiral ones, the second group consists of three and four-legged loaded elements; circular rings; and in the form of square and hexagonal loops, in the third group of solid interior or in various forms, the plate variety is in the form of figures and finally the fourth group is the combinations [1].

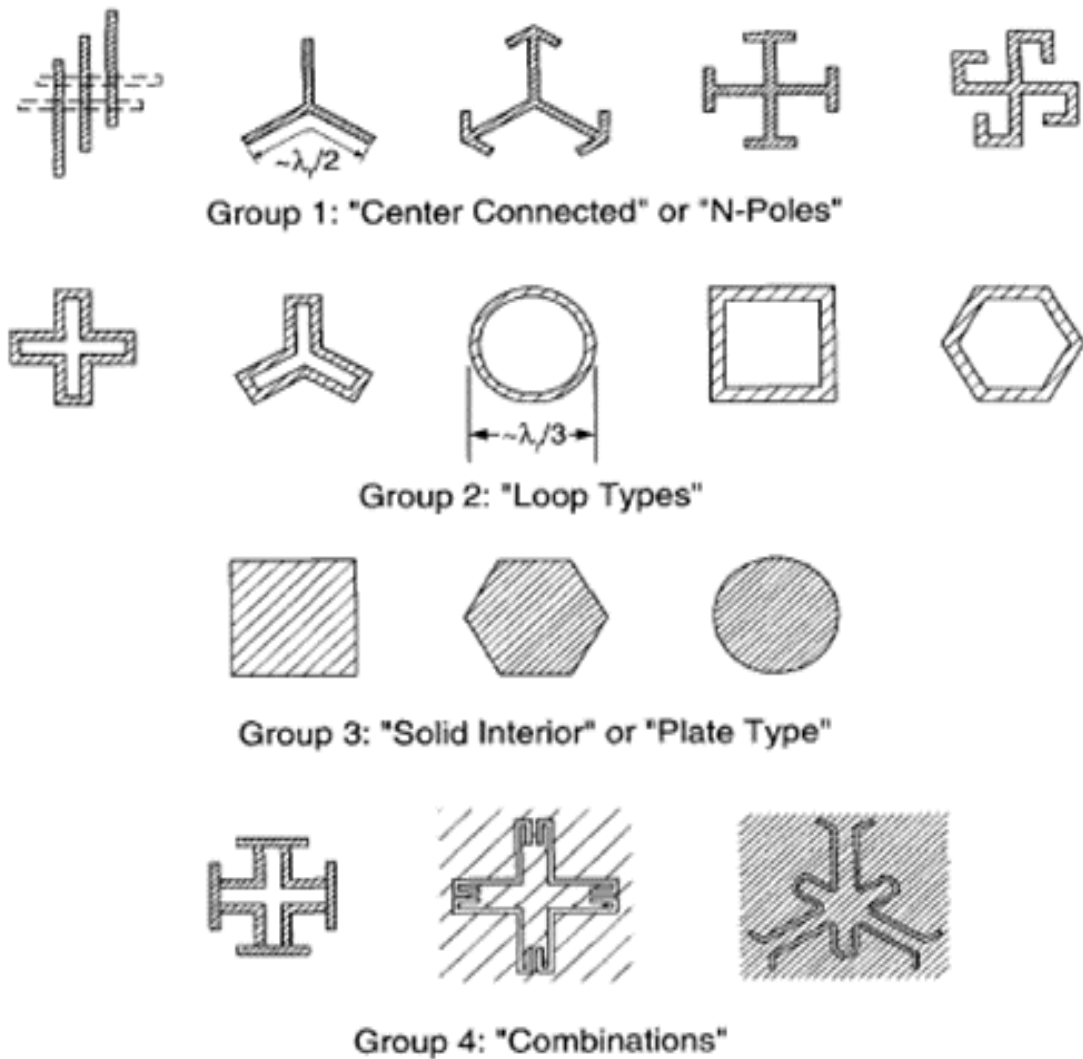


Figure 3.3 : Element type of FSS [1].

The centrally connected structures λ_r (wavelength of the resonance frequency) are approximately twice the length of the dipole, while the wavelengths of the resonance frequency in the loop structures are almost equal to the perimeter of the element [1]. On the other hand, in patch structures, the resonance wavelength will be twice as large as the largest dimension of the geometry. The distance between periodic elements can be at least $\lambda_r / 2$. Hybrid structures are generally the most preferred element geometries that can be changed according to the desired frequency value.

3.2.2 Effect of dielectrics substrate

FSS structures are placed in the dielectric layers when designing. This has two important consequences. The first one is the change of the resonance frequency and the second is the change in the stability of the wave.

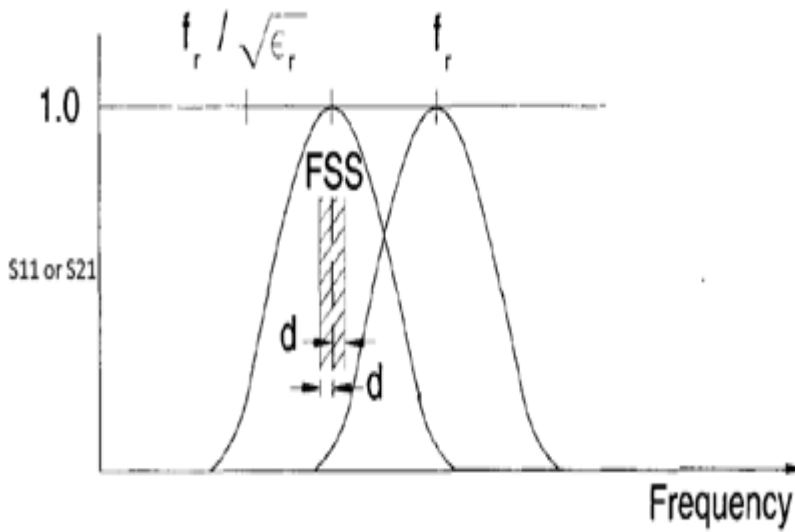


Figure 3. 4 : Effect of dielectric upon the resonant frequency [1].

If the FSS is cover with a dielectric layer with relative dielectric constant ϵ_r , the resonance frequency will change as shown in Figure 3.4 [1].

$$f_{new} = \frac{f_r}{\sqrt{\epsilon_r}} \quad (3.1)$$

If the single side of the FSS is covered with an infinite-wide dielectric layer, then the form of the new resonance frequency will change as follows;

$$f_{new} = f_r / \sqrt{\epsilon_r + 1/2} \quad (3.2)$$

While f_r equal to the resonance frequency, f_{new} equal to new resonance frequency.

The periodic geometry distance (w) change according to the equation of " $w \cdot \cos\theta$ " depending on the angle of incidence of the electromagnetic wave. Resonance frequency and bandwidth of FSS are affected by the incidence angle of the electromagnetic wave [1].

As shown in Figure 3.5, electromagnetic waves coming to the dielectric surface are broken according to Snell law and come to FSS with a narrower angle. Frequency stability of FSSs increases due to the reduced incidence angle.

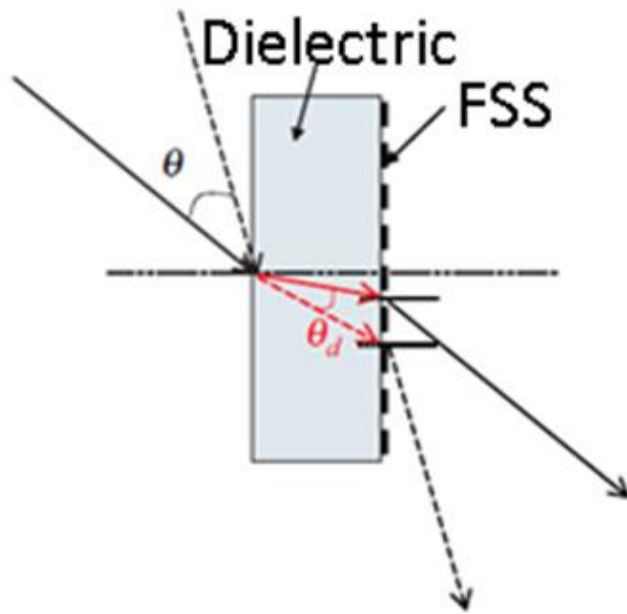


Figure 3. 5 : FSS on the dielectric layer

3.2.3 Grating lobes

When the phase difference between the waves emitted from neighboring elements is 2π and multiples, side beam propagation occur in unwanted directions in FSS.

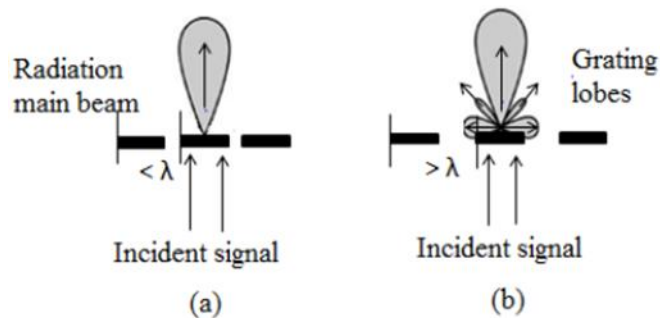


Figure 3. 6 : Grating Lobes (a) period $< \lambda$ (b) period $> \lambda$ [17]

Figure 3.7 shows a plane wave event on a one-dimensional periodic structure with interelement spacing D_x . When the electromagnetic wave on the periodic elements comes with “ η ” angle, a phase difference in “ $\beta \cdot D_x \cdot (\sin(\eta) + \sin(\eta_g))$ ” between adjacent elements occurs.

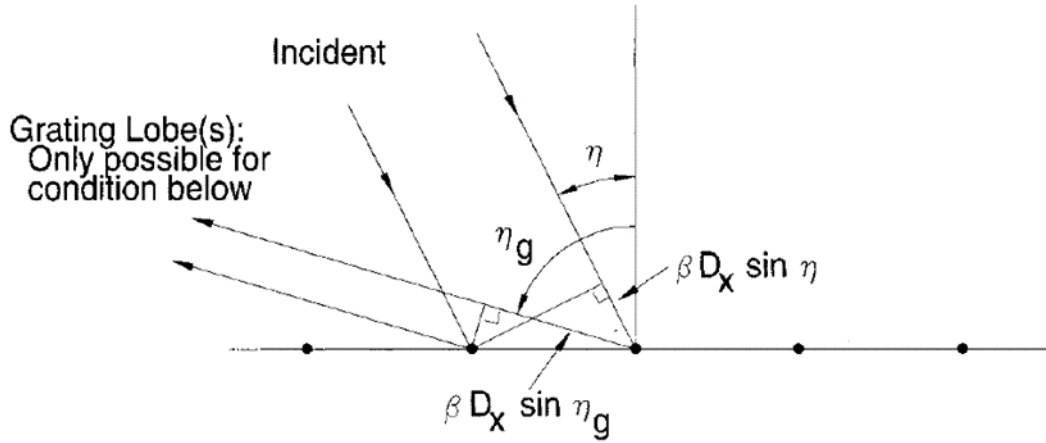


Figure 3. 7 : Occurrence of unwanted propagations [1].

3.3 Analysis Methods of FSS

Various methods are used to perform the analysis while performing FSS design. These methods can be grouped under five headings. These are Method of Moments, Finite Element Method, Finite Difference Time Domain Method, Mutual Impedance Method and Equivalent Circuit Method. While these methods are needed time for simulations, Equivalent circuit method is useful for quickly predicting the performance of FSS.

3.3.1 Finite difference time domain method

The FDTD method was first proposed by Yee in 1966. The application of this method to the periodic surfaces was carried out by Tsay and Pozar. FDTD method started with Ampere law. Then, different formulations were developed for dielectric and metal structures. Over time, both constructs are modeled as follows in a single formula.

$$\varepsilon(\omega) = 1 + \sum_{p=1}^p \frac{b_p}{d_p - \omega^2 + j\omega C_p} \quad (3.3)$$

Where P is the total number of different species or mechanisms, C equals units of radian frequency, also b and d equal units of radian frequency squared. b , d and C depend on the electromagnetic properties of the specific material. Refractive index for

two different material types is expressed by $\epsilon(w)$ [18]. The advantage of the FTDT method does not transform the matrix to solve easy problems [19].

3.3.2 Finite element method

This method started to be applied to electromagnetic problems in 1968. It has been widely used in FSS problems in later years. This method can be easily used in complex geometries and different environments [20]. However, high calculation quality is required for fem to perform mathematical solutions.

3.3.3 Methods of moment

Moment method is used to solve differential field equations used in electromagnetic fields. It is common technique used to solve various scattering problems. Also, transmission and reflection properties for FSS can be found easily with this method. This method uses the Green function [21] for calculations. When a thickness is defined in the multi-layered FSS structures, the solution of the Green function becomes difficult. Therefore, the design for three-dimensional structures is realized and the function becomes more difficult to edit [22].

3.3.4 Mutual impedance method

The mutual impedance approach which sometimes called the element to element method developed by Ben A. Munk. At the same time, scattered waveform of FSS structures can be calculated by this method. The analysis is carried out by obtaining a common impedance expression based on the voltage induced by the electromagnetic wave on the conductive periodic structures and the voltage induced by the other elements on that element [1].

3.3.5 Equivalent Circuit Method

While performing the analysis of FSS, the equivalent circuit method is one of the most preferred methods due to its easy to understand. Equivalent circuit with selected lumped elements can be describe reactance and mutual coupling in structures [23]. This method enables the modeling of the surfaces used as a circuit with inductive and capacitive elements.

Analytical formulas can be used as a function of the impedance behavior of surfaces; for this reason, it has attempted to derive theoretical formulas that predict the frequency behavior of these structures over time.

3.3.5.1 Equivalent circuit method with FSS analysis

According to Marcuvitz's book [24], he developed an equivalent circuit model in which an infinite number of parallel conductive bands are represented for FSS structures. In this model, FSS are composed of inductive and capacitive elements in the transmission lines.

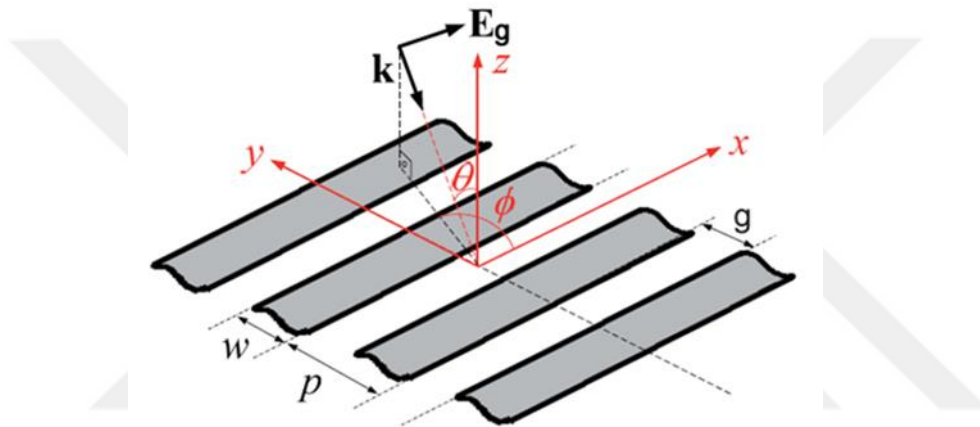


Figure 3. 8 : Periodic structure of parallel metal grids [24]

As shown in Figure 3.8, the planar wave comes with θ and ϕ angle. When the tangential components of the electric field of the incoming wave are in the direction of the metal grids, the periodic structure allows very little conduction at low frequencies, but also shows an inductive characteristic that permits transmission at high frequencies. Equivalent circuit model is drawn with an inductive element of short-circuit to ground in the transmission lines whose characteristic impedance is equal to the characteristic impedance of the gap. The transmission coefficient of the FSS structures determines the grid width (w), periodic distance (p), incidence wave angles (θ, ϕ) and polarization.

When the thickness of the metal strips used is zero, the width w , the wavelength λ and the periodicity is considered to be p ,

The inductive equivalent reactance;

$$\frac{X_L}{Z_0} = F(p, w, \lambda, \theta) = \frac{p \cos\theta}{\lambda} \left\{ \ln \left[\operatorname{cosec} \left(\frac{\pi w}{2p} \right) \right] + G(p, w, \lambda, \theta) \right\} \quad (3.4)$$

Where,

$$G(p, w, \lambda, \theta) = \frac{0,5(1 - \beta^2)^2 \left[\left(1 - \frac{\beta^2}{4} \right) (C_+ + C_-) + 4\beta^2 C_+ C_- \right]}{\left(1 - \frac{\beta^2}{4} \right) + \beta^2 \left(1 + \frac{\beta^2}{2} + \frac{\beta^2}{8} \right) (C_+ + C_-) + 2\beta^6 C_+ C_-} \quad (3.5)$$

$$C_{\pm} = \frac{1}{\sqrt{1 \pm \frac{2p \sin\theta}{\lambda} - \left(\frac{p \cos\theta}{\lambda} \right)^2}} - 1 \quad (3.6)$$

$$\beta = \sin\left(\frac{\pi w}{2p}\right) \quad (3.7)$$

In a similar way, the incident magnetic field vector is parallel to the metal strips and it illuminates the array with an angle φ . The strips have periodicity, p , and a gap between the strips, g . The capacitive susceptance is calculated by [24]:

$$\frac{B_C}{Z_0} = 4F(p, w, \lambda, \theta) = \frac{4p \cos\theta}{\lambda} \left\{ \ln \left[\operatorname{cosec} \left(\frac{\pi w}{2p} \right) \right] + G(p, w, \lambda, \theta) \right\} \quad (3.8)$$

The inductive equivalent reactance formulation and the capacitive susceptance formulation are determined by the wavelengths and incidence angles between the ranges: $p(1+\sin\theta)/\lambda$ [25].

3.3.5.1.1 Equivalent circuit method analysis for the square loop

The square loop samples and equivalent circuits models used in the literature are shown in Figure 3.9.

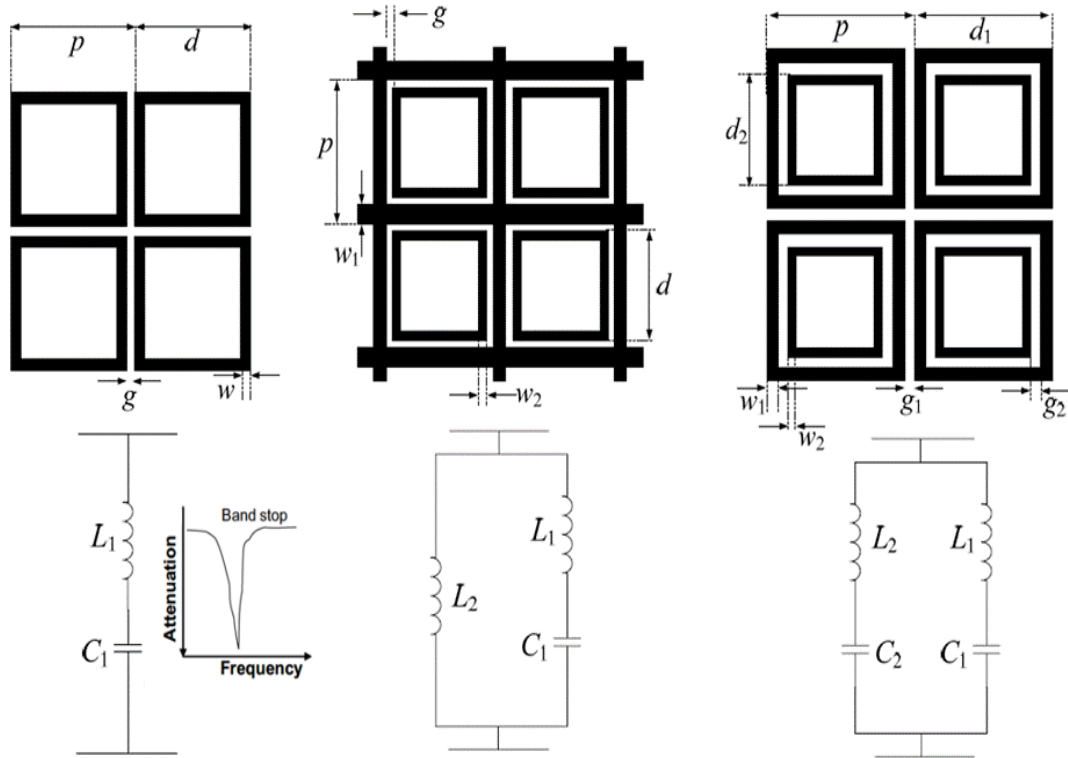


Figure 3. 9 : Square loop FSSs, parameters and equivalent circuit models [26]

Based on the planar wave transmission responses, there is a single reflection band in the structure given in Figure 3.9 (a). The second structure shows a more frequent frequency response than first structure. The band centers of these structures do not change according to the incidence angle, but the bandwidths can give different values. The final structure consists of four interlocking square loops. So, it occurs both a high frequency transmission band and a low frequency reflection band are formed. [26].

The mathematical calculation of the equivalent circuit model given in Figure 3.9 (a) is as follows [27].

$$Y = \frac{1}{B_1 + X_1} \quad (3.9)$$

$$B_1 = \omega C_1 = 4.0 F(p, g, \lambda)(d/\varepsilon_r p) \quad (3.10)$$

$$X_1 = \omega L_1 = F(p, 2w, \lambda)(d/p) \quad (3.11)$$

The second calculation of the equivalent circuit model given in Figure 3.9 (b) is as follows;

$$Y = -j \left(\frac{1 - \omega^2 C_1 (L_1 + L_2)}{\omega L_2 (1 - \omega^2 C_1 L_1)} \right) \quad (3.12)$$

The finally calculation of the equivalent circuit model given in Figure 3.9 (c) is as follows;

$$Y = j\omega \left(\frac{C_1 + C_2 - \omega^2 C_1 C_2 (L_1 + L_2)}{1 - \omega^2 C_1 L_1 (1 - \omega^2 C_2 L_2)} \right) \quad (3.13)$$

3.3.5.1.2 Equivalent circuit method analysis for the jerusalem cross

The Jerusalem cross structures are widely used in the literature as square loop. Figure 3.10 demonstrate this structure and equivalent circuit models of this structure.

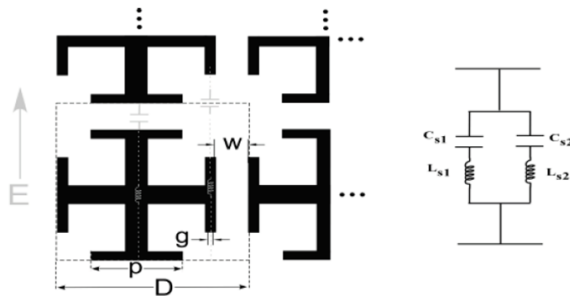


Figure 3. 10 : Jerusalem Cross FSS parameters and equivalent circuit model [28]

This model allows to increase the capacitance value due to its structure. The structures found at the endpoints are considered as loading dipoles, so a LC circuit is added in addition to the original circuit.

The impedance of the circuit;

$$Z_{LC\parallel LC} = \frac{(1 - \omega^2 L_{S1} C_{S1})(1 - \omega^2 L_{S2} C_{S2})}{j\omega(C_{S1} + C_{S2} - \omega^2 C_{S1} C_{S2} (L_{S1} + L_{S2}))} \quad (3.14)$$

$$C_{S1} = \frac{1}{L_{S1} \omega_{z1}^2} \quad C_{S2} = \frac{1}{L_{S2} \omega_{z1}^2} \quad (3.15)$$

$$L_{S2} = \frac{\left(\frac{\omega_{p2}^2}{\omega_{z2}^2}\right) L_{S1} C_{S1} - \left(\frac{1}{\omega_{z2}^2}\right)}{C_{S1} \left(1 - \frac{\omega_{p2}^2}{\omega_{z2}^2}\right)} \quad (3.16)$$

The first pole ω_{p1} falls at $\omega=0$ since the FSS is capacitive.

3.4 Application Areas of FSS

The use of FSS has increased in many applications such as satellite communication, artificial magnetic conductor design, high selective spatial filter [2], microwave polarization converter, dichroic reflector surfaces, and subreflector design for large aperture antennas. All FSS structure designed during the thesis study were developed for use as a sub-reflector in reflector antennas. The frequency selective surface is placed between the two feeders of the reflective antenna. Feeder number 1 shows transmission capability at the operating frequency (f_1), while feeder number 2 shows the reflection in operating frequency (f_2). As a result, this structure allows the reflective antenna to radiate at two different frequencies [1].

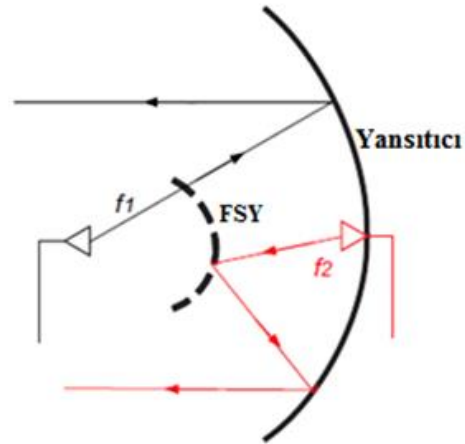


Figure 3. 11 : A double-band reflective antenna [29].

The subreflector does not necessarily have to be a hyperboloid, it can be flat as shown in Figure 3.12. The design of the flat reflector is always easier than the design of the convex reflector but the important part in the design is that the mechanical shapes of all the reflective surfaces need to be protected.

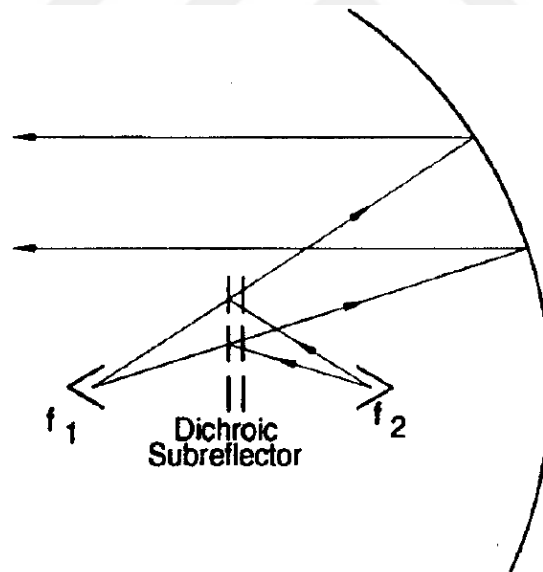


Figure 3. 12 : A double band reflective antenna created using a flat reflector [1].

One of the second most important areas of application is the use of FSSs to reduce the radar cross-section of the antennas outside the working areas. RCSs have become more advantageous to use FSS structures so it was difficult to control at wide frequency with antennas [30]. The radome structure of the hybrid antenna, which is one of the radom applications, is given in Figure 3.13.

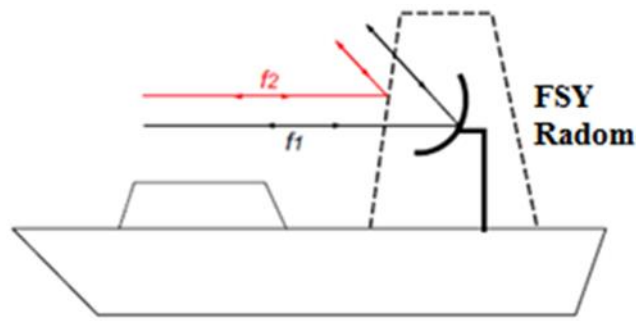


Figure 3. 13 : Hybrid antenna radome [29]

In order to increase the efficiency of the antennas in this application, the radomes are covered with FSSs reflecting the other markings that pass the markings on the working frequency [1].

Another application is demonstrated in Figure 3.14. FSS structures used in this application work as a polarizer. Linear polarized and 45° curved event wave is separated into two components, horizontal and vertical. these components recombine into a circular polarizing wave after passing through the polarizer. Cascading two or more polarizer sheets can improve the bandwidth. When a dielectric layer is added, the angle of incidence stability can increase [1].

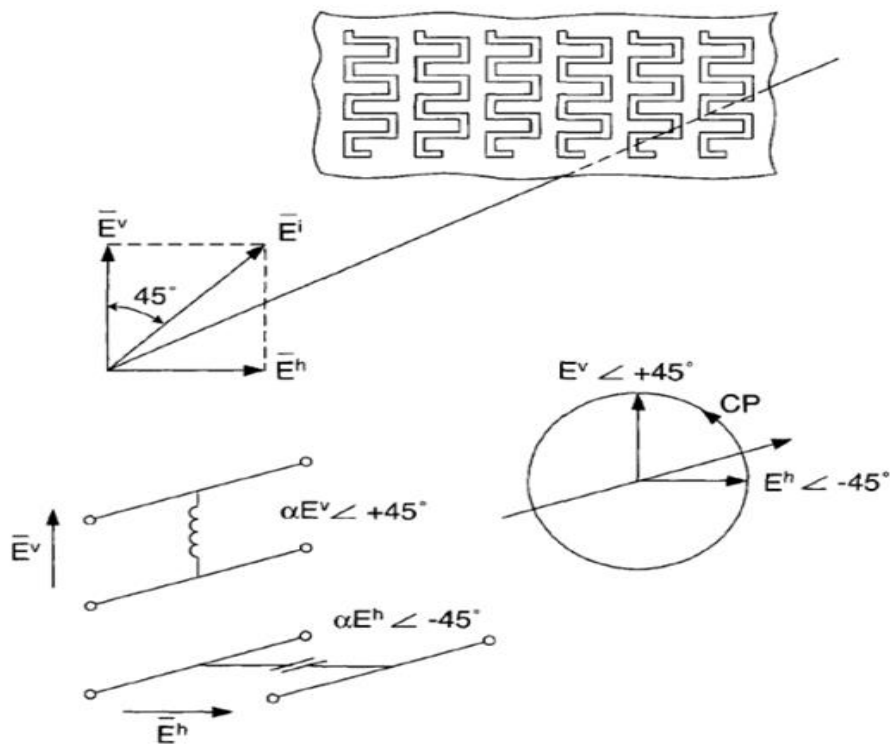


Figure 3. 14 : Use of FSSs as polarizers [1]

3.5 Use of FSS in Reflector Antennas

In Chapter 2, reflector antennas commonly used in satellite applications are mentioned. In this section, reflector antennas with multiple working bands will be described. In the literature, the use of frequency selective surfaces as sub-reflectors in the design of reflector antennas having more than one working band is widely preferred [31,32,33]. Figure 3.15 shows an example of the use of FSS as a sub-reflector. Two feed antennas are used in this structure. The one feed placed at the center of the parabola is used for Ka / X band, while the other feed placed behind fss is used for Ku / S band. While the fss for the feed placed in the center of the parabola exhibits band-stop behavior, the same fss shows band-pass behavior for other feed. Due to the frequency selective surface, this structure shows the Cassegrain antenna feature in the X and Ka band. It also features an axis-symmetric parabolic reflector antenna in the S and Ku band.

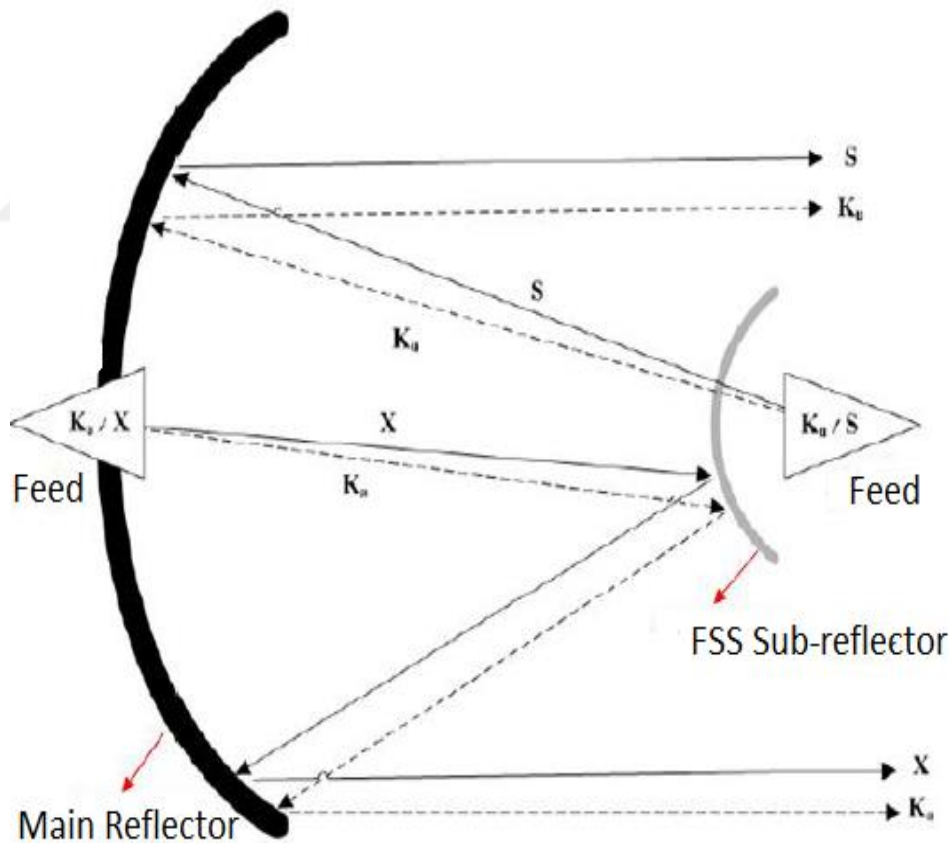


Figure 3. 15 : Reflector antenna structure with multiple working bands [39].

The use of fss models designed in this thesis study in reflector antennas are shown in Figure 3.16, Figure 3.17 and Figure 3.18, respectively.

The model given in Figure 3.16 is created for the fss described in section 4.1. FSS, which is used as a sub-reflector in this structure, stops the Ka band signals from the feed so the signals radiate from the main reflector.

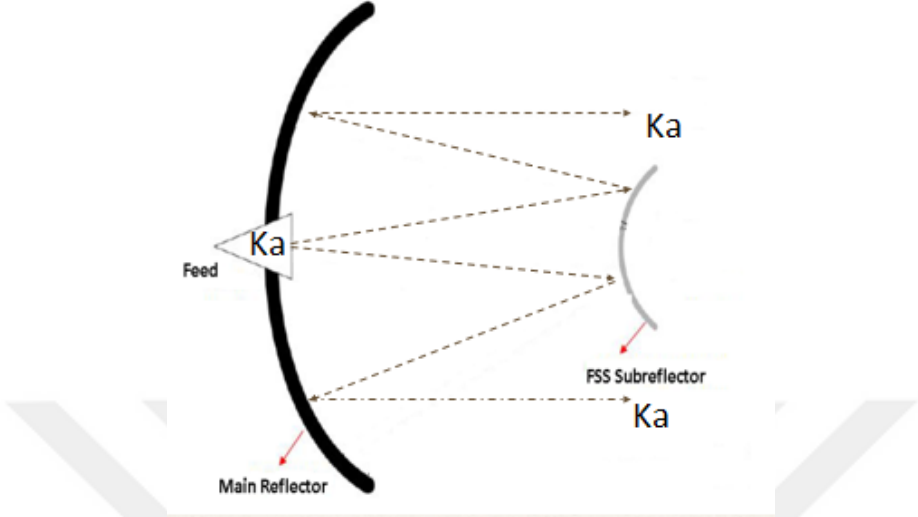


Figure 3.16 : Reflector antenna design for Ka band signals with subreflector FSS

The model given in Figure 3.17 is created for the fss described in section 4.2. As shown in Figure 3.17, both X-band and Ka-band feeds are used. The purpose of this design is to reduce the number of feeds in multi-band structures. At the same time, it is not necessary to choose the mechanical structures used for feed with this structure.

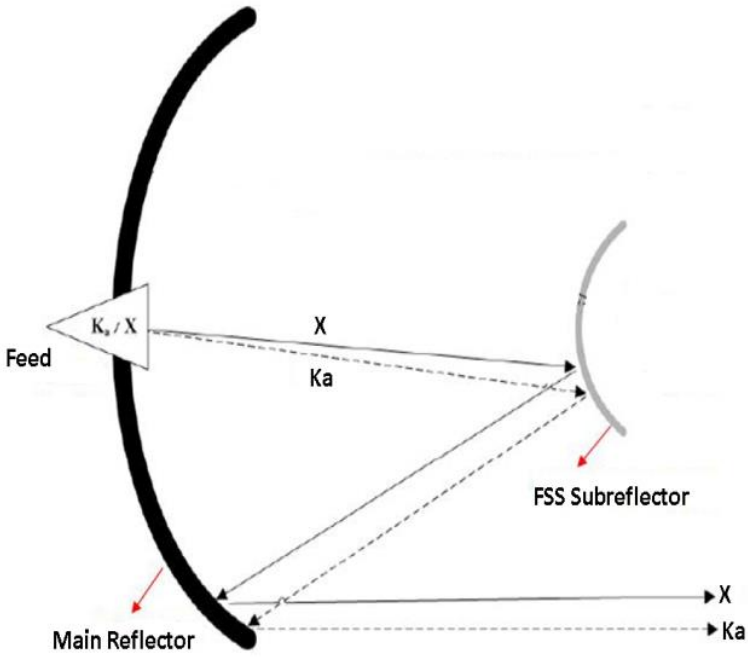


Figure 3.17 : Reflector antenna design for Ka band and X band signals

The last model given in Figure 3.18 is designed for the fss described in section 4.3. The aim of this model is to design an FSS that will work as a sub-reflector using Ka band (26.5 – 40 GHz) and Ku (12- 18 GHz) band frequency range. The designed FSS in Chapter 4.3 can be used in reflector antennas with one feed in Ku and Ka band. For this structure, a single feed may be preferred instead of using more than one feed and mechanical feed structure.

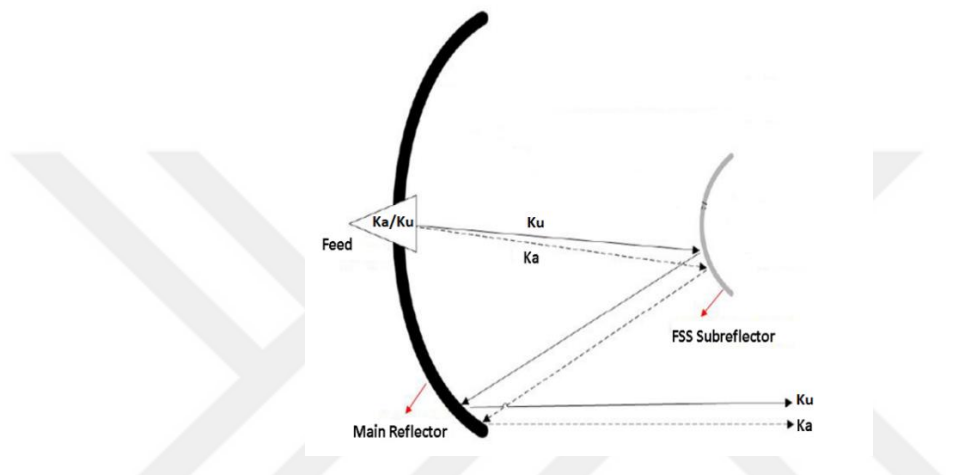


Figure 3. 18 : Reflector antenna design for Ka band and Ku band signals

3.6 Manufacturing Methods of FSS

The printing of the conductive periodic structures used in the FSS design is carried out on the dielectric layers. When the electrical properties and dimensions of the dielectric layers change, the frequency characteristics of the FSSs change. It is desired that the electrical properties of the dielectric layer used are constant and that the temperature dependence is not high.

3.6.1 Implementation of FSS prints on FR4 layer

Screen printing (silk printing) is a technique that allows printing on all kinds of surfaces such as metal, ceramic, fabric, glass and plastic. The companies that produce electronic cards produce electronic circuit printing on copper-coated FR4 dielectric sheets with this technique. FR4 is a fireproof dielectric layer obtained from the woven of glass yarns with epoxy resin. It is used in the production of printed circuit boards in electronics with the copper coating.



4. DESINGS

The purpose of the thesis is a frequency selective surface design which does not pass the signals from the Ku, Ka and X bands. The designed structure in this study is expected to stop the desired frequency bands at least -10 dB. In this thesis, three different designs are realized. Firstly, in terms of simplicity, only an FSS which has a band stopping characteristic is designed in the multiple resonance regions of the Ka band. In this design described in section 4.1, a new FSS structure is designed which is different from the literature which has band stop capability at the desired frequencies up to 60-degree incidence angle for a single band. As a result of this design, transmission coefficient parameters are examined for both TE and TM modes.

Secondly, the frequency selective surface designs with band stop characteristic in more than one frequency band have been realized. In the first of the multi-band FSS designs, FSS structures designed for X band are investigated. The FSS structures which have band stop characteristics are designed with different geometries for both X band and Ka band. After that, these two different geometries in these two different cells are combined in a single cell. When the simulation results are examined, it is observed that approximately 2 GHz shift in both TE and TM modes in the only Ka band depending on the incidence angle. According to this result, the miniature geometry used for the Ka band change the frequency response depending on the incidence angle, but there is no change in the X band.

In the final stage of this thesis study, it is aimed to solve the problems come across in the above-mentioned designs and to realize a new design that can be used as a sub-reflector in satellite applications. For this design, Ka and Ku band, which are the two frequencies most used in satellite communication, are preferred. The cell size of the proposed structure is " $0.2\lambda \times 0.2\lambda$ ". When the results are evaluated, it is understood that this structure has high selectivity, a small size and miniaturized structures. Moreover, TE and TM modes show a stable response up to 60 degrees of incidence angle. In this design study, S_{11} parameter results are evaluated at the same time.

According to these results, it was clearly observed that the FSS structure works as a band stop rather than as an absorber.

The structures designed in this thesis are explained below, respectively.

4.1 Design 1: A Novel Multi-Band FSS for Ka-Band Applications

In this study, dual-band FSS design consisting of only one layer is proposed for to use as a sub-reflector in reflector antenna designs in satellite communication applications. Proposed FSS reflects Ka band (25.5-27.3 GHz and 41.8-45.1 GHz) signals and have a stable frequency response up to 60 degrees of incidence angles. Maximum reflection is achieved at 25.7 and 43.2 GHz frequencies. Proposed design provides high frequency selectivity, easy fabrication and stable frequency response for Ka-band satellite applications.

In the proposed hybrid design is shown in Figure 4.1. Three- armed geometry is placed in the center and two armed geometries are placed in each quadrant of the unit cell in order to reflect the incoming waves in 26.5 GHz frequency band. Two-legged geometries are placed in corners and square loop geometries are placed in each quadrant of the unit cell in order to reflect the incoming waves in 40 GHz frequency band.

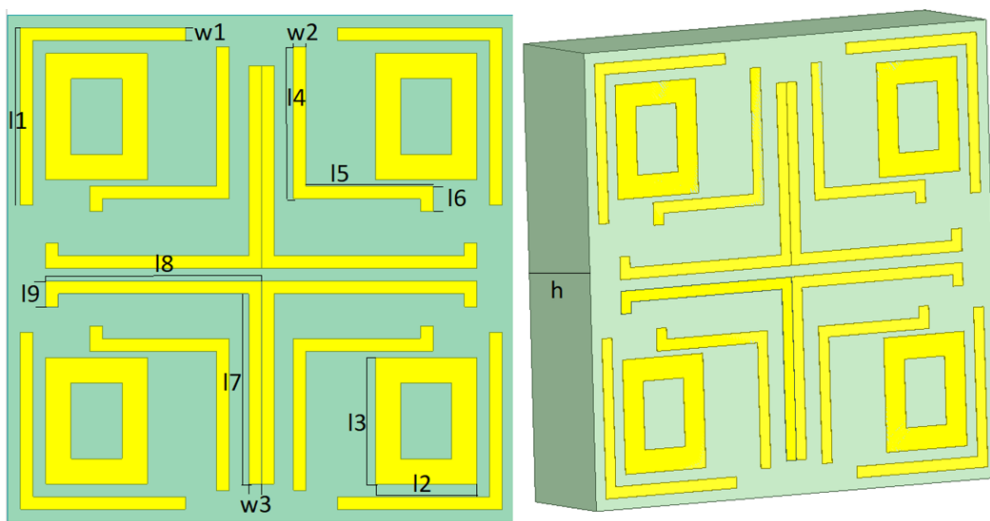


Figure 4. 1 : Geometry of FSS element

Design parameter values are given in Table 1. Unit cell dimension are 3.72 mm x 3.72 mm. 1 mm (h) FR4 substrate is used in the design with permittivity of $\epsilon_r = 4.4$ and loss tangent of 0.02.

Table 4.1 : Parameter values of first FSS.

Parameter	Value(mm)
h	1
w1	0.09
w2	0.09
w3	0.09
l1	1.3
l2	0.743
l3	0.921
l4	1.116
l5	0.93
l6	0.18
l9	0.18
l7	1.4
l8	1.581

The FEM-based cell analysis method in the HFSS is used for the simulation process during the design stage. To obtain the results of the analysis of the designed FSS under ideal conditions, the periodic elements are defined as excellent conductors as shown in Fig. 4.2. Then, a vacuum box is created that covers the unit cell.

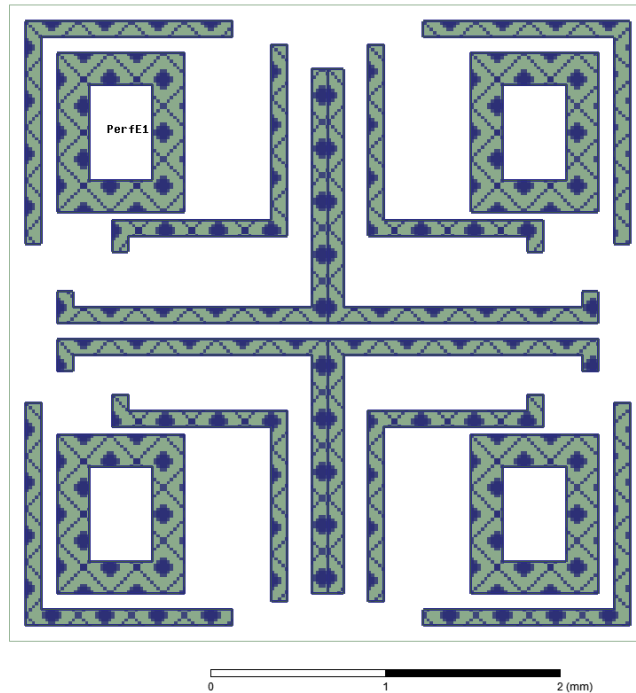


Figure 4. 2 : Boundary conditions for surface

Simulation of the designed unit cell as an infinite array either in one or two dimensions is provided by the master and slave boundary conditions in HFSS as shown in Fig. 4.3. The phase difference between master and slave is evaluated.

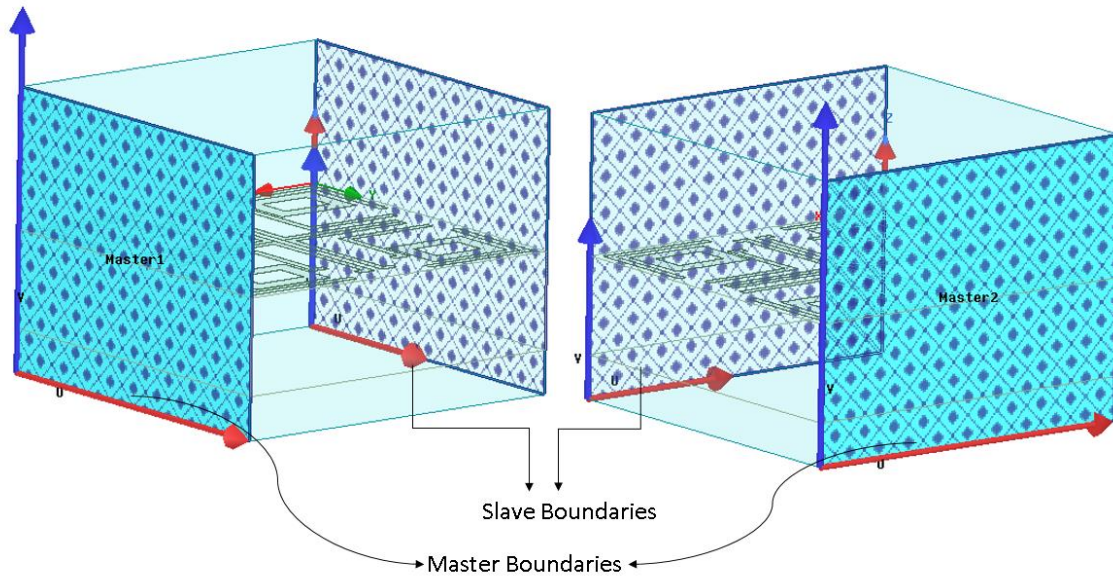


Figure 4.3 : Master and Slave boundary conditions

The wave port must be selected after the master slave boundary conditions have been set. There are three wave ports in the HFSS program such as Wave port, Lumped Port, and Floquet port. Wave port is used for microstrip, stripline, coaxial, or waveguide transmission lines. A wave port determines the area or region where the source is connected. In addition, this port is the excitation which is applied over a cross-sectional area. This port is limited by PEC boundary conditions. So, the wave port should be resized according to the design of the structure. The lumped port is mainly used as a wave source in transmission lines. Lumped ports that can be used in simulations where energy needs to be sourced internally to a model. The most difference between lumped port and wave port, while the lumped port is assigned to the internal face of the design, wave port is assigned to the external face. Floquet port is used in the simulation of planar and periodic structures. Floquet modes are plane waves with propagation direction set by the frequency, phasing, and geometry of the periodic structure. Floquet modes also have propagation constants such as wave modes. Floquet ports are used as shown in Figure 4.4 to send the electromagnetic wave to the unit cell model. The waves sent by the floquet port occur a phase difference between the walls and the unit cell.

In order to evaluate both transmission and reflection characteristics in the fss structures, two floquet port are placed above and below the unit cell.

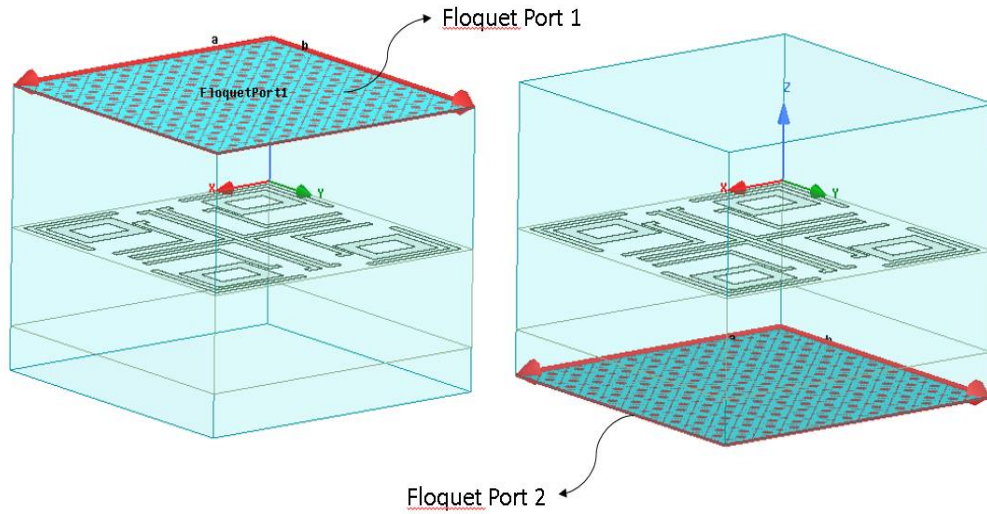


Figure 4. 4 : Floquet port for a unit cell in HFSS

Two basic modes for evaluating simulation results are examined. These modes are TE (Transverse electric) and TM (Transverse magnetic). With these modes, the scattering of electromagnetic waves over the frequency selective surface can be evaluated. Finally, the result of the analysis was evaluated by parameters S_{21} (transmission coefficient) and S_{11} (reflection coefficient). The design and optimization processes for all the designed structure were carried out in the same program and with the same process steps. Transmission coefficients of the designed FSS structures are simulated different angles (0° to 60°) for TE and TM polarizations. Simulation results are demonstrated in Fig.4.5 and Fig. 4.6.

Simulation results for TE polarization show that proposed FSS is capable of reflecting the incoming electromagnetic waves in Ka band, especially at the 26.5 GHz and 43.4 GHz center frequencies. Besides, obtained reflection losses in 26.5 GHz and 43.4 GHz frequency bands are 0.44 dB and 0.5 dB, reflectively. In addition, 7.5% and 7.4% of reflection bandwidths are achieved at 26.5 GHz and 43.4 GHz frequency bands, respectively for 60 degrees of incidence angles. Since the designed structure is not exactly symmetrical, different simulation results are obtained in TE and TM modes.

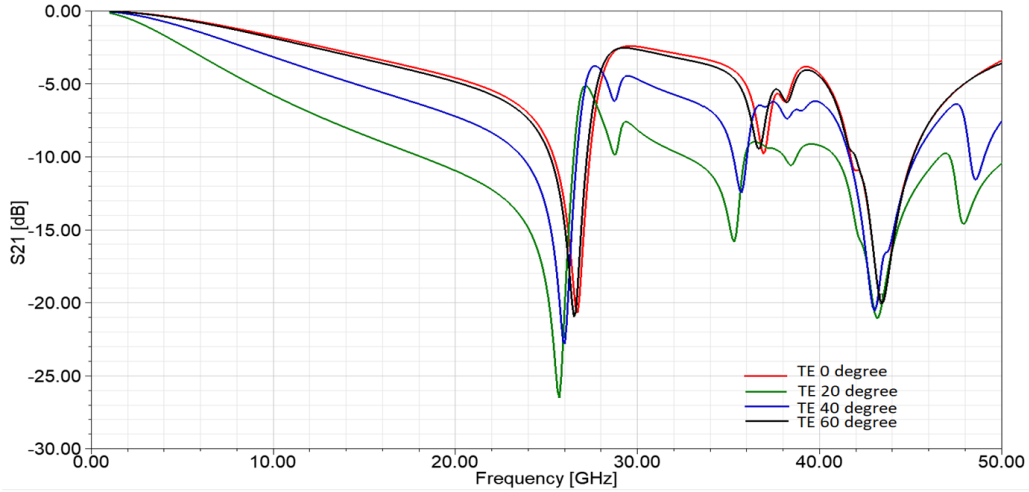


Figure 4. 5 : S_{21} frequency for the first FSS geometry, TE polarization.

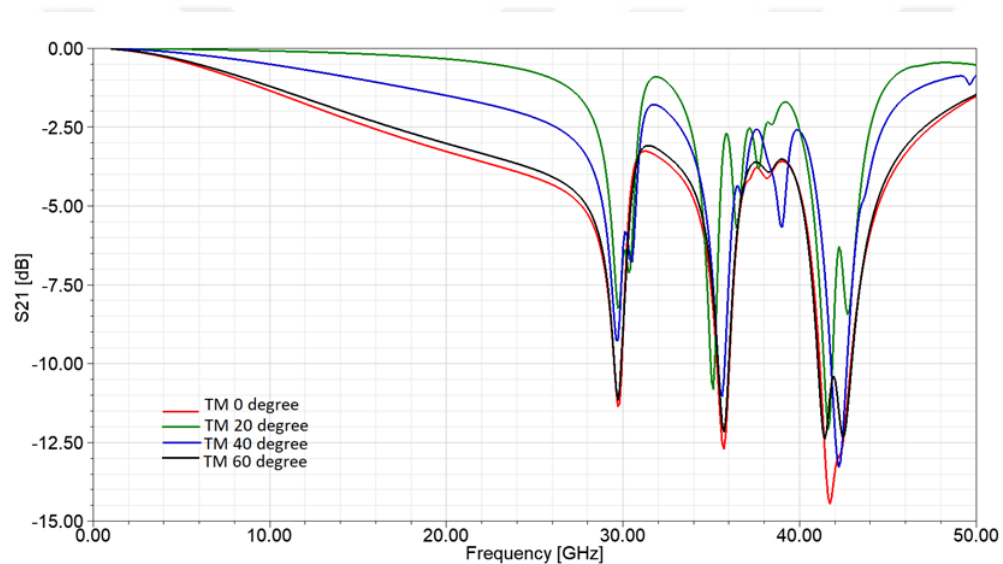


Figure 4. 6 : S_{21} frequency for the first FSS geometry, TM polarization.

On the other hand, TM simulation results show three reflection bands at 29.7 GHz, 35.6 GHz and 41.7 GHz frequencies. Achieved reflection losses are less than 0.5 dB in the desired frequency bands for all incidence angles. In addition, 1.3% and 4.3% of reflection bandwidths are achieved at 29.7 GHz and 41.7 GHz frequency bands, respectively for 60 degrees of incidence angles. It can also be seen that the transmission coefficients are below -10 dB in the desired frequency bands for incident angles ranging from 0° to 60° for both TE and TM polarizations.

This work is published in “The Seventh International Conference on Telecommunication and Remote Sensing – ICTRS’18”.

4.2 Design 2: A Miniaturized Dual Ka/X Band Frequency Selective Surface

Figure 4.7 shows a single layer FSS structure designed to stop the Ka band and X band frequency ranges. The values of the geometries used in the designed structure are given in Table 4.2. For this structure, unit cell size is "5 mm x 5 mm". Proposed FSS consist of one FR-4 substrate layer. In this symmetrical design, a center placed three-line structures are employed to reflect Ka band signals and an outer ring structure is employed to reflect X band signals.

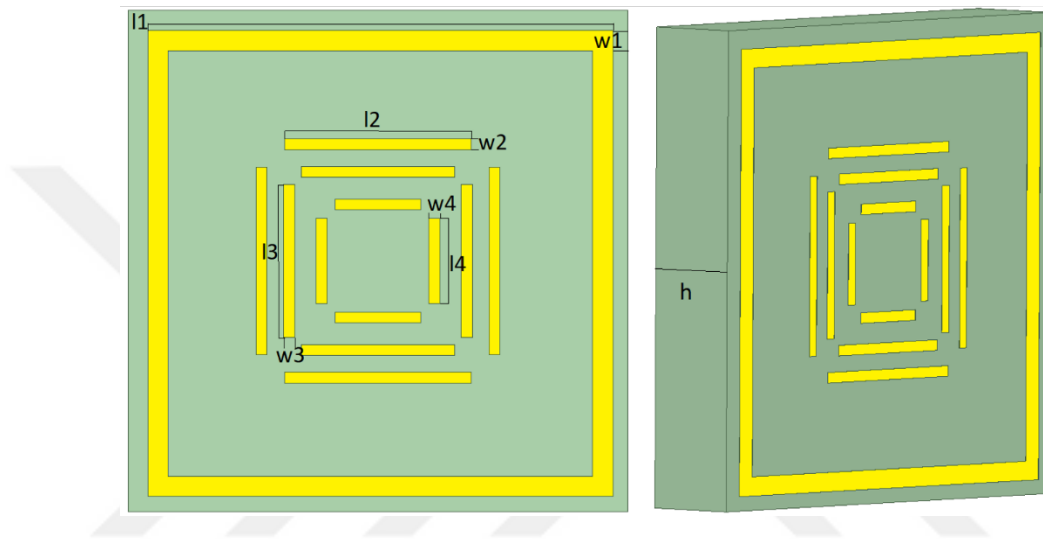


Figure 4. 7 : Geometry of second FSS element

Table 4.2 : Parameter values of second FSS.

Parameter	Value(m m)
h	1
w1	0.11
w2	0.11
w3	0.11
w4	0.11
l1	4.65
l2	1.87
l3	1.53
l4	0.85

When it is desired to design an fss with more than one stop band, multiple layers are used to increase stability. However, in this study instead of multilayered structures, fss

structure with multiple stop bands are designed in a single layer. The design consists of three stages. First stage, a ring geometry is used to accomplish a reflection in X band. Second stage, a center placed three-line structures is designed and optimized to achieve a reflection in Ka band. Last stage, these two structure are combined in one unit cell to design a multi-band structure. Simulation results for the all structure is given Figure 4.8, 4.9 and 4.10 .

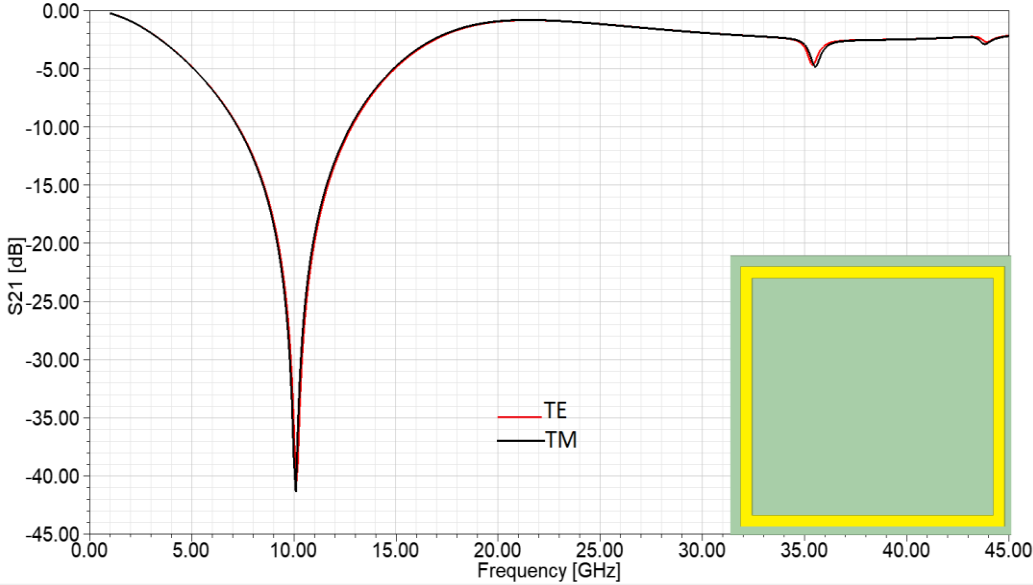


Figure 4. 8 : S_{21} frequency curves for the first design stages of second FSS

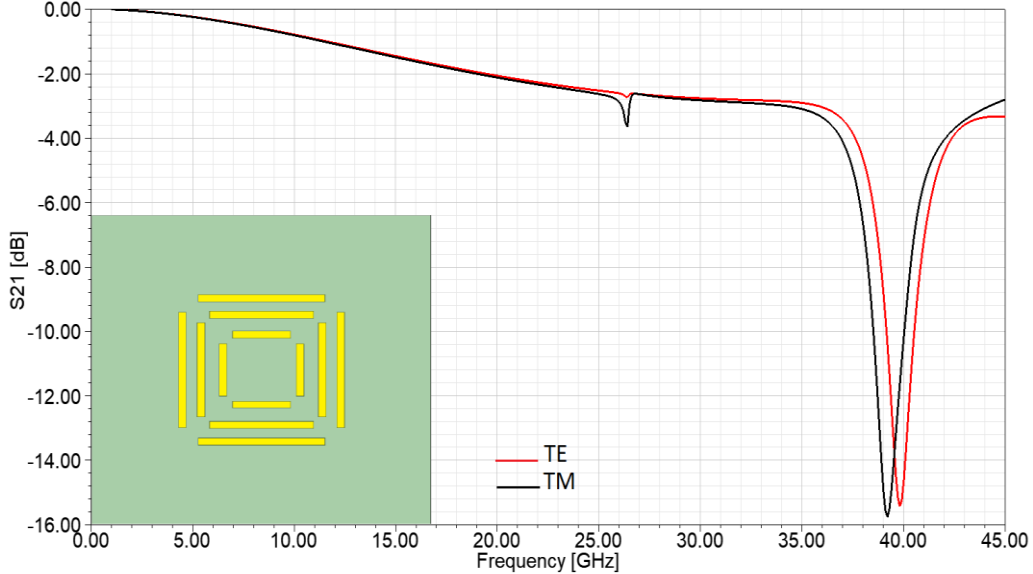


Figure 4. 9 : S_{21} frequency curves for the second design stages of second FSS

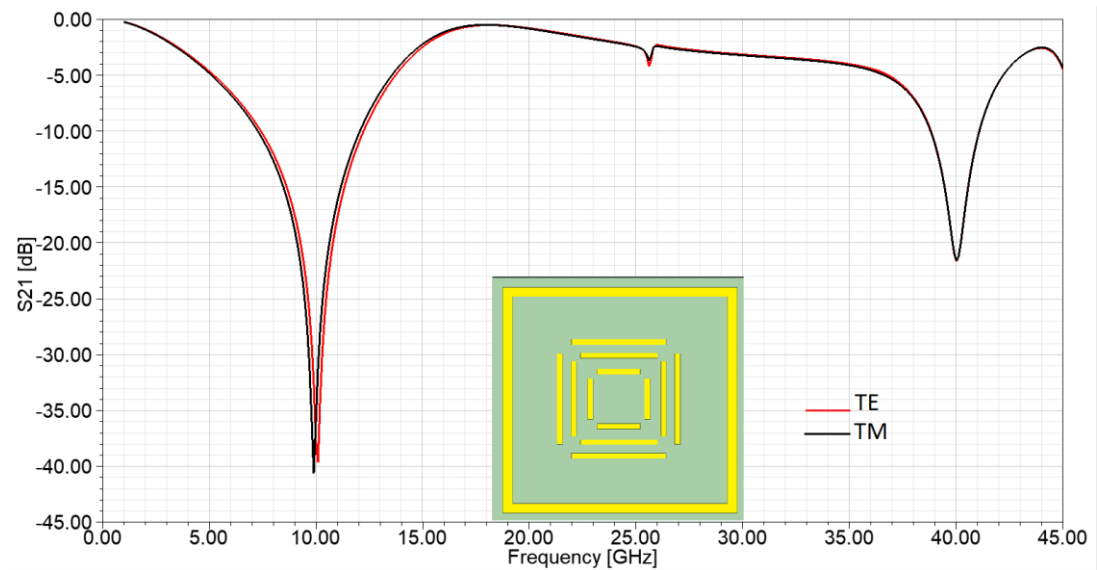


Figure 4. 10 : S_{21} frequency curves for the last design stages of second FSS

As seen from the above results, the two bands used don't affect each other and good results are obtained.

Transmission coefficients (S_{21}) of the final FSS structure is simulated for different incidence angles (0° to 60°) at TE and TM polarizations. Achieved results (Figure 4.11 and Figure 4.12) show that transmission coefficients are below -10 dB in Ka and X bands for incident angles ranging from 0° to 45° for both TE and TM polarizations.

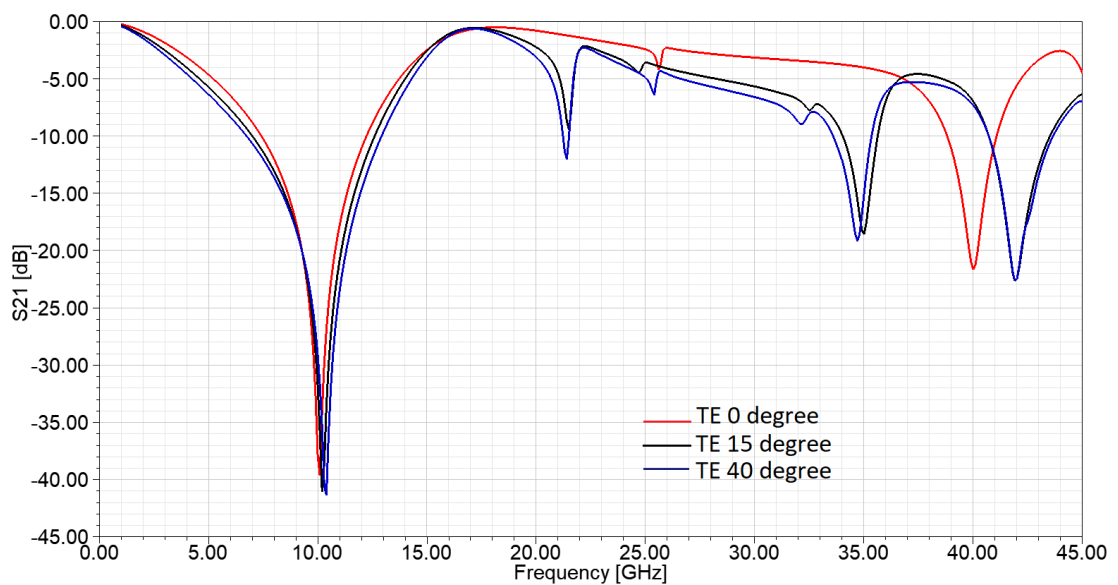


Figure 4. 11 : S_{21} frequency for the second FSS geometry, TE polarization

For TE polarization, simulation results show that designed FSS reflects the incoming electromagnetic wave in X band covering 8-12 GHz. In the Ka band, four different reflection frequency band is observed at the 34.7 GHz, 35 GHz, 40 GHz, 42 GHz center frequencies. When these results are evaluated, it is observed that the Ka band, which is one of the stop bands, has approximately 2 GHz shift in both TE and TM mode. The geometry structure designed for the X band shows continuity, while the geometric structures designed for the Ka band are miniaturized and do not show continuity. This is the reason for the 2 GHz shift in the results.

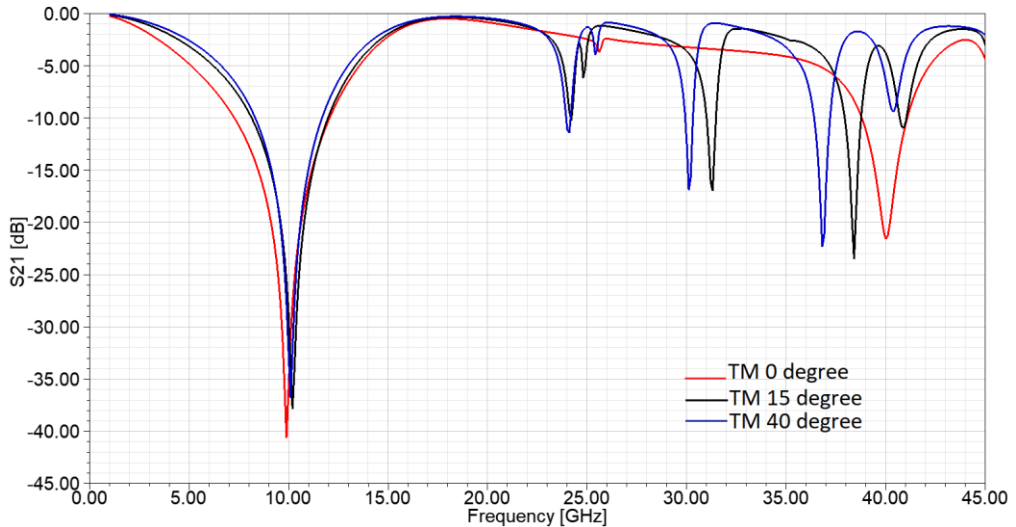


Figure 4.12 : S_{21} frequency for the second FSS geometry, TM polarization

On the other hand, achieved reflection losses in 10 GHz and 40 GHz frequency band are less than 0.06 dB and 0.1 dB, as shown in Figure 4.13. Besides, 46% and 5.25% of reflection bandwidths are achieved at 10 GHz and 40 GHz frequency bands, respectively at 0 degree of incidence angle.

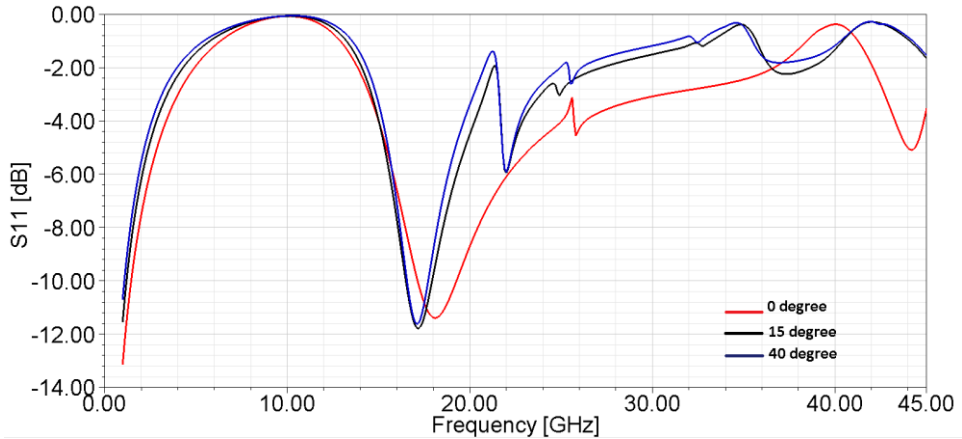


Figure 4.13 : S_{11} frequency for the second FSS geometry

Simulation results for TM polarization demonstrate that designed FSS is capable of reflecting the incoming electromagnetic waves in X and Ka bands, especially at the 10 GHz, 30 GHz, 31 GHz, 36.8 GHz, 38.4 GHz, 40 GHz center frequencies. In addition, obtained reflection loss in 10 GHz and 40 GHz frequency bands are less than 0.1 dB for 0 degree of incidence angle. 48% and 5.75% of reflection bandwidths are achieved at 10 GHz and 40 GHz frequency bands, respectively for 0 degrees of incidence angle. It can be also shown in Fig.4.11 and Fig.4.12 that almost same bandwidths are achieved at the 10 GHz and 40 GHz center frequencies for TE and TM polarizations.

This work is published in “The 3rd International Mediterranean Science and Engineering Congress- IMSEC”.

4.3 Design 3: A Dual- Band FSS Design for Satellite Applications

In this design, FSS acting a sub-reflector has been designed to be a reflective layer for Ku and Ka feeds. With this design, the antenna can be used to receive electromagnetic waves in different polarization in the two desired frequency band. Therefore, the communication capacity of the antenna systems in satellite communication systems can be increased while the mass and volume of the satellite payload can be reduced. The designed FSS model reflects both Ku band (14.8-16 GHz) signals and Ka band (33-36 GHz) signals for an oblique angle of incidence for dual polarization with stable performance. This design is to have maximum reflection at 15.5 GHz and 35.3 GHz. The geometry of the proposed unit cell is given in Figure 4.14.

The dimensions of the unit cell are 4mm x 4mm and thickness is $h=1$ mm. While a center placed four arm structure is designed for Ku band, two-legged structures placed in corners and four leg structures placed in each quadrant are designed for Ka band. The size of the unit cell for the lower frequency is $0.2\lambda \times 0.2\lambda$, where λ refers to free space wavelength. The cell consist of one substrate layer including FR4 material with permittivity $\epsilon_r = 4.4$, loss tangent of 0.02.

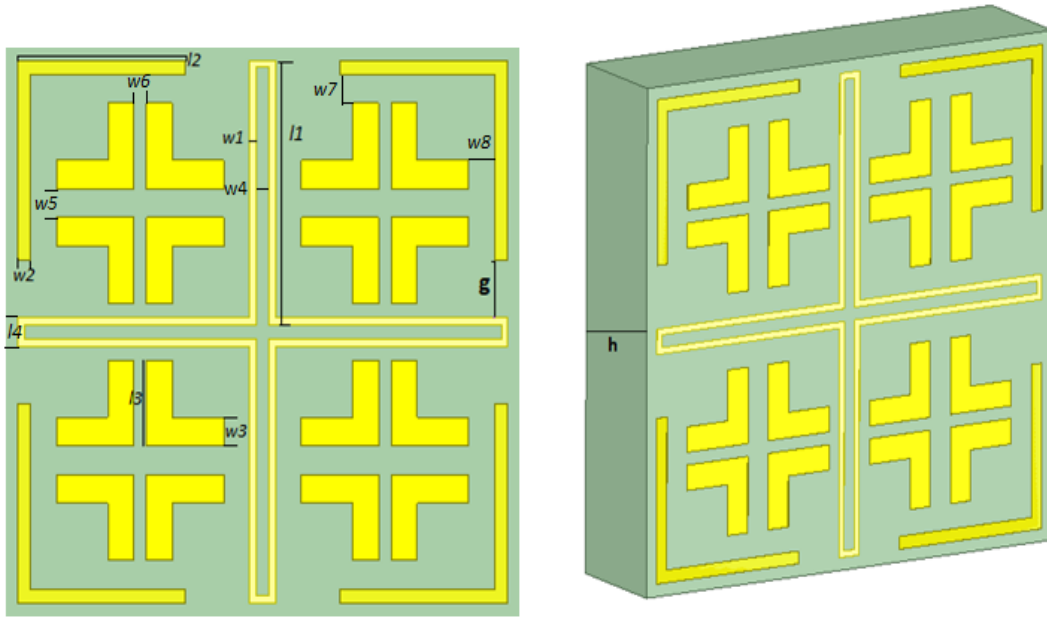


Figure 4.14 : Geometry of third FSS element

Parameter values of the unit cell for the final FSS structure are shown in Table 4.3. “h” and “g” parameters denote the thickness of FR4 substrate and the gap between the periodic elements, respectively.

Table 4.3 : Parameter values of last FSS.

Parameter	Value(mm)
h	1
g	0.5
l1	1.85
l2	1.3
l3	0.6
w5	0.2
w7	0.2
w8	0.2
l4	0.2
w1	0.05
w2	0.1
w3	0.2
w4	0.1
w6	0.1

The reflection band in Ku band is controlled by length l1 and patch width w1, while in Ka band it is determined by two-legged structures placed in corners that have length l2 and width w2.

Another four leg structures placed in each quadrant are symbolized by the width w_3 of length l_3 . Stopband can be controlled individually by lengths l_1, l_2, l_3 and widths w_1, w_2, w_3 . The design process is demonstrated in Figure 4.15, Figure 4.16, Figure 4.17, respectively. Firstly, it is tried to design an FSS for Ku band. When the results of the designed structure are evaluated, the structure shows reflection characteristic at both 15 GHz and 30 GHz range.

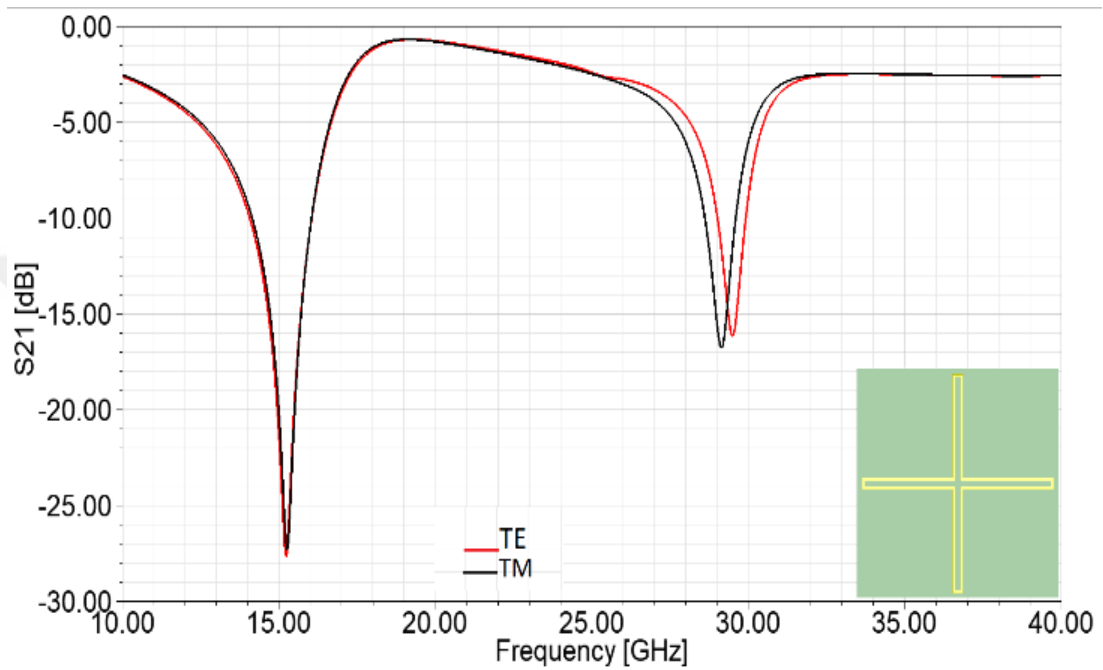


Figure 4. 15 : S_{21} frequency for the first design stages of the third FSS

But, the desired frequency is 35 GHz for Ka band. So, four leg structures placed in each quadrant is added to assess the desired frequency value in Ka band. According to the results seen in Figure 4.16, the frequency value is shifted but the desired S_{21} parameters could not be satisfied in the Ka band. Finally, we placed two-legged structures in the corners as the last patch cell and desired parameters are obtained.

As shown in Figure 4.18 and Figure 4.19, three different patch units are placed in the periodic cell to obtain double reflection band response with angle and stability. By changing w_1, w_2 and w_3 values in the patch cells, simulation procedures are repeated and the variations of these changes in the frequency values are examined.

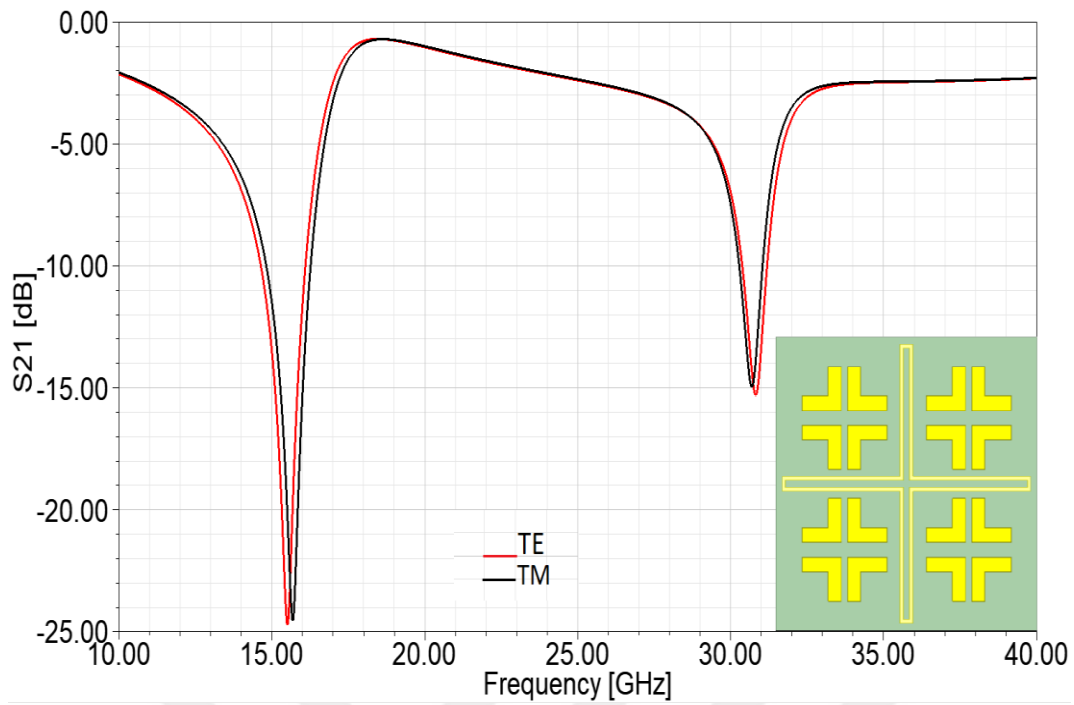


Figure 4. 16 : S_{21} frequency for the second design stages of the third FSS

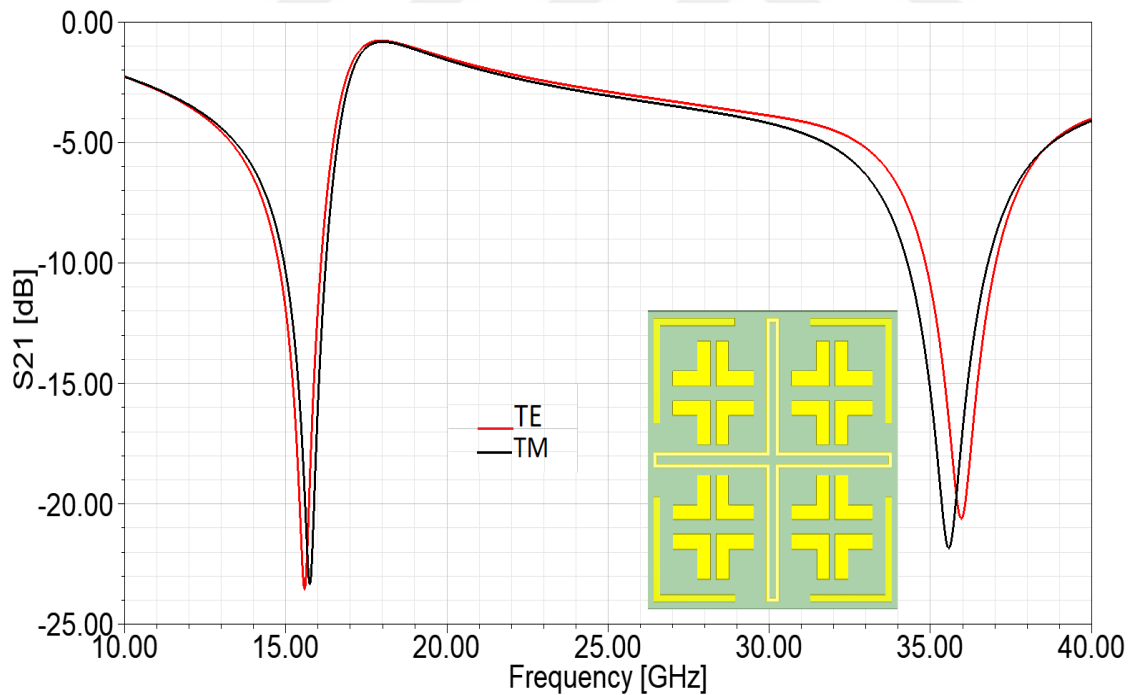


Figure 4. 17 : S_{21} frequency for the second design stages of the third FSS

In order to be able to change the w_1 , w_2 and w_3 values randomly, the equivalent circuit model which is one of the most preferred methods in the literature has been used.

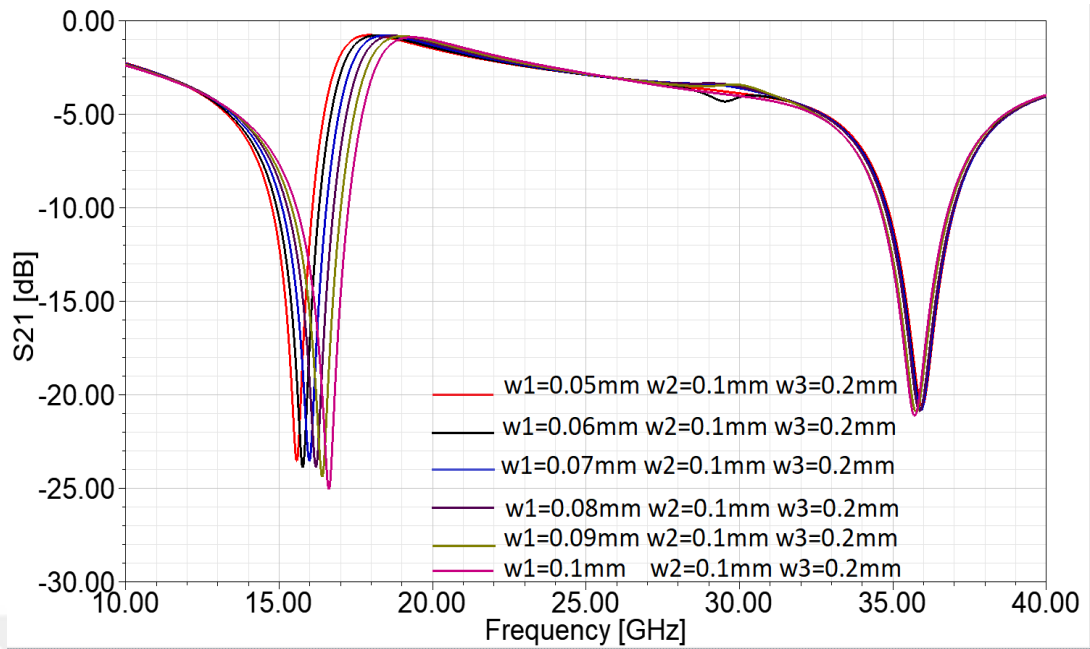


Figure 4. 18 : S_{21} frequency for the different value of the parameters including w_1

In the use of the equivalent circuit model in the HFSS simulation program, firstly the minimum and maximum w value ranges are defined . Then, this program increases the selected values in the desired range to find the best-performing parameter.

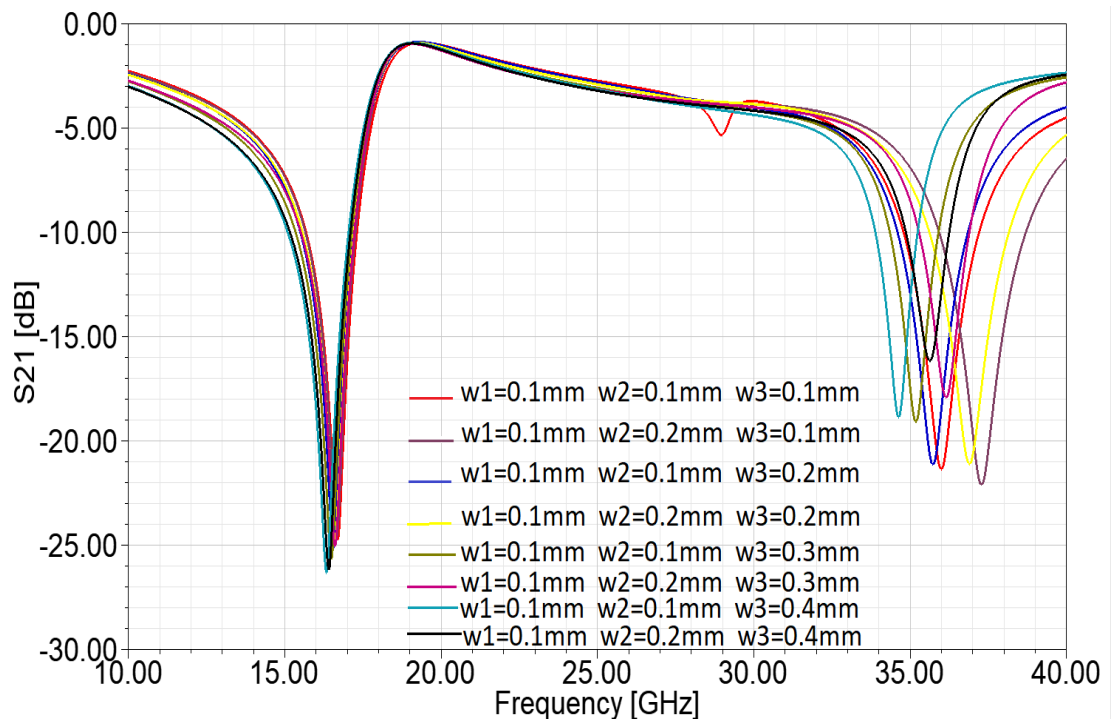


Figure 4. 19 : S_{21} frequency for the different value of the parameters

FSS geometry can be represented with an equivalent circuit (EC) model as seen in Figure 4.20. Z_0 represents the free space characteristic impedance. The width of the gap (s) and the gap (g) between conducting geometries primarily determine the equivalent capacitance ($C \propto \frac{d}{w}$). The length (d) and the width (w) of the current path primarily determine the equivalent inductance ($L \propto \frac{d}{w}$) of periodic element geometries. Each resonator (15 and 35 GHz) of the FSS structure acts as a reflector for the desired frequency bands and can be modeled by a serial LC circuit. The coupling effect between the resonators is represented by a mutual inductance.

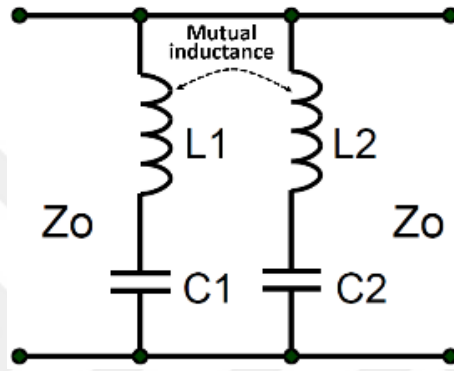


Figure 4. 20 : EC model of FSS structure

Equivalent impedance and resonance frequency of the FSS can be derived from the circuit model as:

$$Z = \frac{(1 - w^2 L'_1 C_1)(1 - w^2 L'_2 C_2)}{jw(C_1 + C_2 - w^2 C_1 C_2 (L'_1 + L'_2))} \quad (4.1)$$

$$L'_1 = L_1 - M, L'_2 = L_2 + M \quad (4.2)$$

$$f_{15GHz} = \frac{1}{2\pi\sqrt{L'_1 C_1}}, f_{35GHz} = \frac{1}{2\pi\sqrt{L'_2 C_2}} \quad (4.3)$$

Desired frequency response can be obtained by changing the element dimensions of the periodic structure considering the relationships between the equivalent capacitance and inductance values and element geometry.

Simulated transmission coefficients for different angles (θ from 0° to 60°) of TE and TM polarizations are demonstrated in Fig.4.21 and Fig.4.22. As shown in Fig. 4.21 and Fig. 4.22, the transmission coefficients (S_{21}) are below -10 dB for the incident angles from 0° to 60° for both TE and TM polarizations in Ku-band (14.1–16 GHz) and Ka band (29.2- 36.8 GHz), respectively.

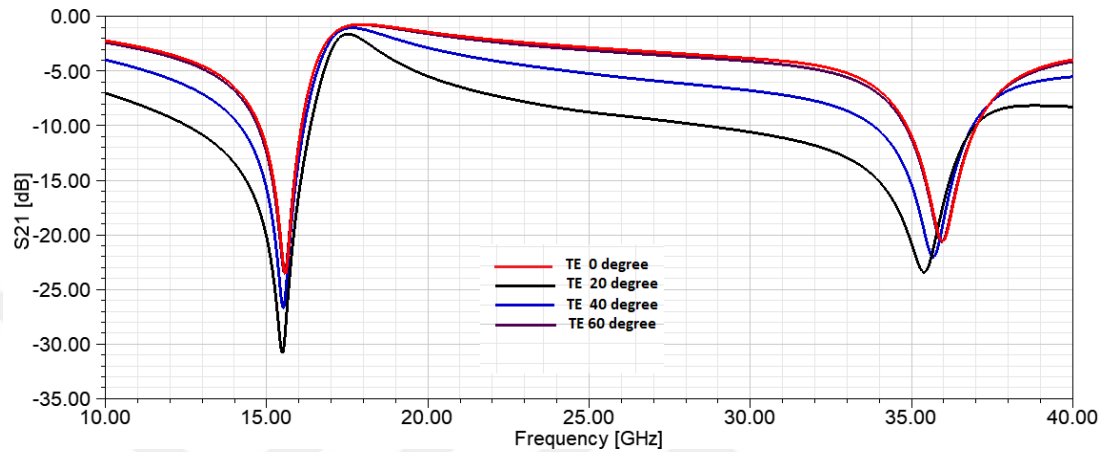


Figure 4. 21 : S_{21} frequency for the third FSS geometry, TE polarization

It is also observed that the transmission parameter (S_{21}) increases with the increase of incidence angles at TE polarization and decreases with the increase of incidence angles at TM polarization, as expected. However, 35 GHz band is less stable than the 15 GHz band for oblique incidence angles due to the distance between 15 GHz resonant geometries in neighboring cells is larger than the 35 GHz geometries.

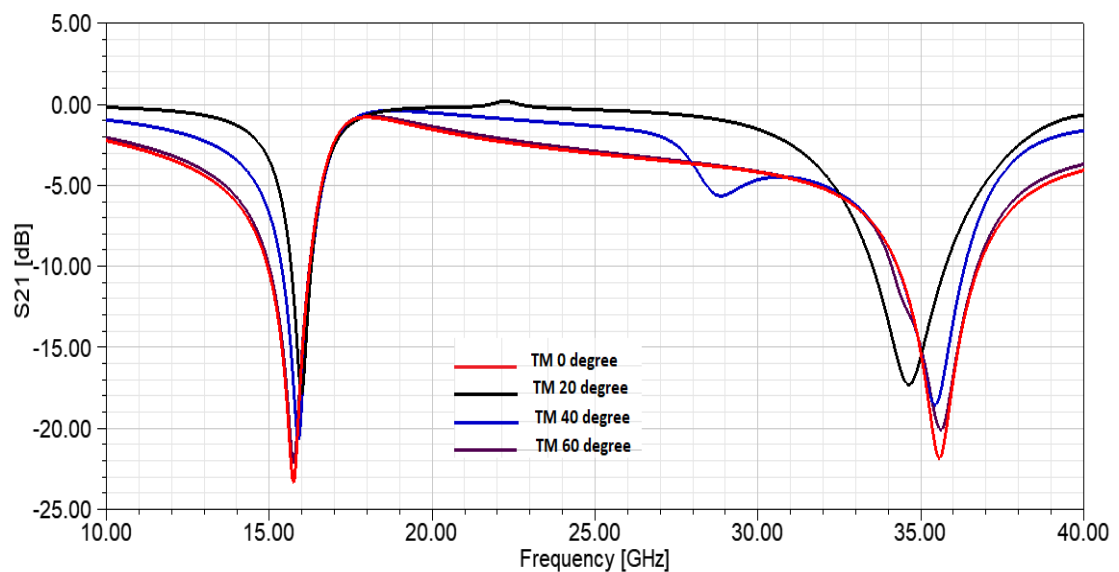


Figure 4. 22 : S_{21} frequency for the third FSS geometry, TM polarization

As shown in Figure 4.23, reflection loss is observed 0.5 dB in 35.3 GHz when TE wave incident is from 0° to 60°. While the bandwidth at 35.5 GHz for TM wave incident angle 0° is 6.8 %, the bandwidth at 36 GHz for TE wave incident angle 0° is 5.7 %. On the other hand, reflection loss is less than 0.6 dB in 15.5 GHz for TM wave incident from 0° to 60°. While the bandwidth at 15.5 GHz for TE wave incident angle 0° is 8.4 %, the bandwidth at 15.76 GHz for TM wave incident angle 0° is 7.6 %.

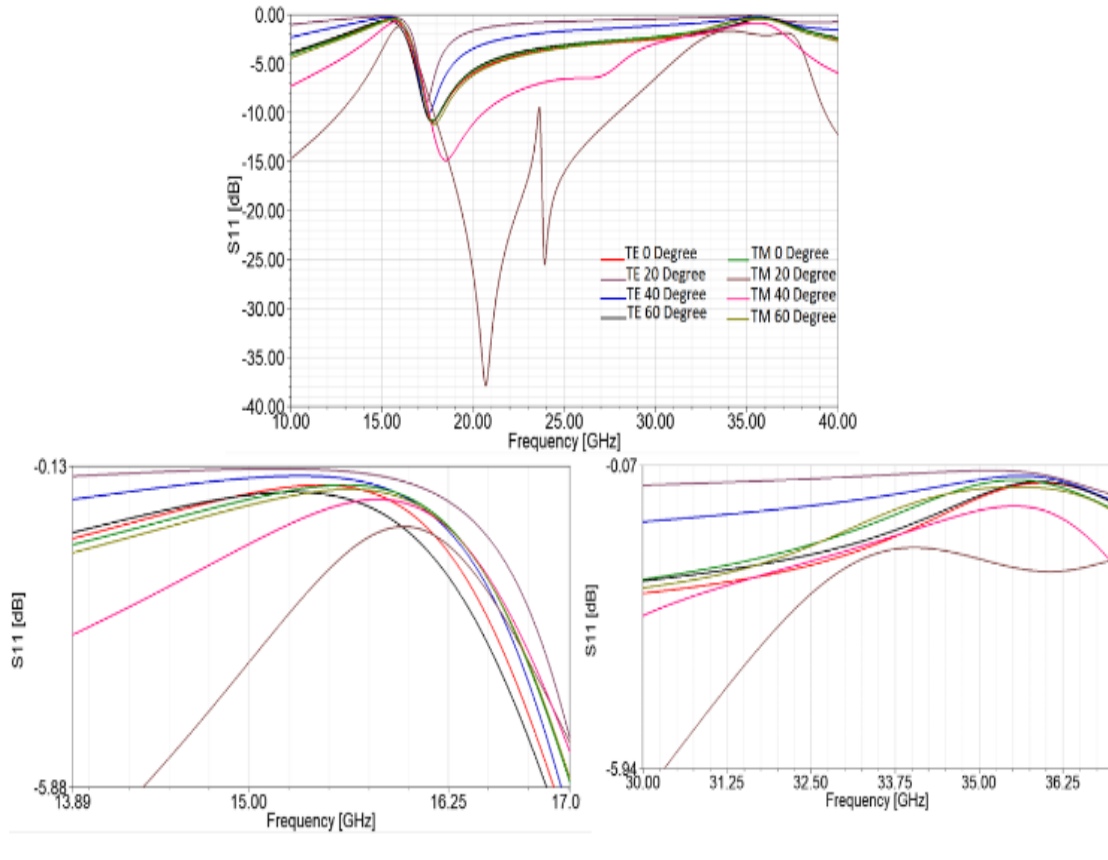


Figure 4. 23 : S_{11} frequency for the third FSS geometry

Table 4.4 compares some parameters of the proposed designed with the other works given in the literature. Unit cell size, operation bands, number of substrate layers, operation frequency bands, polarization and range of incident angle parameters are selected, respectively.

As seen in Table II, the designed FSS structure is more compact size than structures designed in [35] and [36]. Moreover, proposed FSS structure as a single layer has a larger range of incident angle than in [35] and [37]. In addition, this structure has more operation bands than in [37] and [36].

Table 4.4 : Comparasion of the proposed FSS with the similar FSS.

FSS articles	Unit Cell Size	Operation Bands	Number of Substrate Layer	Operation Frequency Bands	Polarization	Angle Range
[35]	1.9×1.9×4	2	4	Ku, Ka	dual	45°
[37]	3×3×4	1	4	K	dual	40°
[36]	6×6×11.5	1	5	Ku	dual	60°
[7]	5×5×0.508	3	1	X, Ku, Ka	dual	80°/80°/60°
This work	4x4x1	2	1	Ku, Ka	dual	60°

This work is published in “The 18th Mediterranean Microwave Symposium – MMS 2018” .

4.4 Comparison of Designs

In this thesis study, single-band and multi-band frequency selective surface designs are performed at Ka, Ka / X and Ka / Ku band frequencies. It is not possible to compare these designs within themselves because each proposed FSS is designed in different frequency ranges. This situation is taken into consideration and FSSs are investigated in the literature and Table 4.5 is prepared.

Table 4.5 : Comparasion of the proposed all FSSs with the similar FSS.

FSS articles	Unit Cell Size	Operation Bands	Number of Substrate Layer	Operation Frequency Bands	Polarization	Angle Range
[5]	16x16x0.5	2	Multilayer	X,Ka	dual	40°
[6]	6.79x6.79x5	2	1	Ku, Ka	dual	60°
[7]	5×5×0.508	3	1	X, Ku, Ka	dual	80°/80°/60°
[8]	4x4x0.125	1	3	Ka	dual	0°
[9]	4.5x4.5x0.5	1	1	Ka	dual	60°
[11]	5x5x0.5	2	3	X,Ka	dual	30°
[35]	1.9×1.9×4	2	4	Ku, Ka	dual	45°
[36]	6×6×11.5	1	5	Ku	dual	60°
[37]	3×3×4	1	4	K	dual	40°
Design1	3.72×3.72x1	1	1	Ka	dual	60°
Design2	5×5x1	2	1	X,Ka	dual	40°
Design3	4x4x1	2	1	Ku, Ka	dual	60°

In this study, the first design works in a single frequency band so this design can be compared to the designs in [8], [9] and [36]. Design 1 has a compact size compared to the design of [8], [9] and [36]. In addition, this design has fewer layers compared to [8] and [36]. Even though operating frequencies in second design same as in [5] and [11], the second design has a smaller cell size than in [5] and [11]. At the same time, the maximum incidence angle of design 2 is higher than in [11] so design 2 is more stable. The designed last FSS is more compact size than structures designed in [35] and [36]. Moreover, proposed FSS structure as a single layer has larger range of incident angle than in [35] and [37]. In addition, this structure has more operation bands than in [37] and [36].

Table 4.6 : S_{21} parameters in the proposed designs for TE

		0°	15°	20°	40°	60°
Design1	26.7 GHz	-20.7 dB	-	-26.5 dB	-22.8 dB	-21 dB
	43.5 GHz	-19.9 dB	-	-21 dB	-20.5 dB	-19.9 dB
Design2	10 GHz	-39.6 dB	-41 dB	-	-41.3 dB	-
	40 GHz	-21.65dB	-18.6dB	-	-19 dB	-
Design3	15.5 GHz	-23.5 dB	-	-30.8 dB	-26.6 dB	-23.5 dB
	35.5 GHz	-20.5 dB	-	-23.3 dB	-22 dB	-20.5 dB

Table 4.7 : S_{21} parameters in the proposed designs for TM

		0°	15°	20°	40°	60°
Design1	35.7 GHz	-12 dB	-	-10 dB	-11 dB	-12.1 dB
	41.7 GHz	-15 dB	-	-12 dB	-13 dB	-12.3 dB
Design2	10 GHz	-40.6 dB	-37.8 dB	-	-36.8 dB	-
	40 GHz	-21.6 dB	-23.4 dB	-	-22.3 dB	-
Design3	15.5 GHz	-23.3 dB	-	-17.7 dB	-20.5 dB	-22.1 dB
	35.5 GHz	-21.8 dB	-	-17.2 dB	-18.5 dB	-20.1 dB

In Tables 4.6 and 4.7, the parameters of the S_{21} are presented together with the incidence angle for both TE and TM. According to the results in the table the best results are obtained with the third design.

5. FABRICATION AND MEASUREMENTS

Detailed information on the printing of the conductive periodic structures used in the FSS design on the dielectric layers is given in section 3.6. In this section, the materials used in FSS printing and measurement systems will be mentioned. FSS model designed in section 4.3 is fabricated in Mega System. The unit cell in the FSS layer count increased as 50x50. As a result, the layers of FSS are produced in planar dimensions 20 cm x 20 cm by using FR-4 material. FR-4 material is preferred because of both easy to find and cheap. As shown in Figure 5.1, copper material is used for printing geometries. In addition, Figure 5.2 shows a close view of the material.

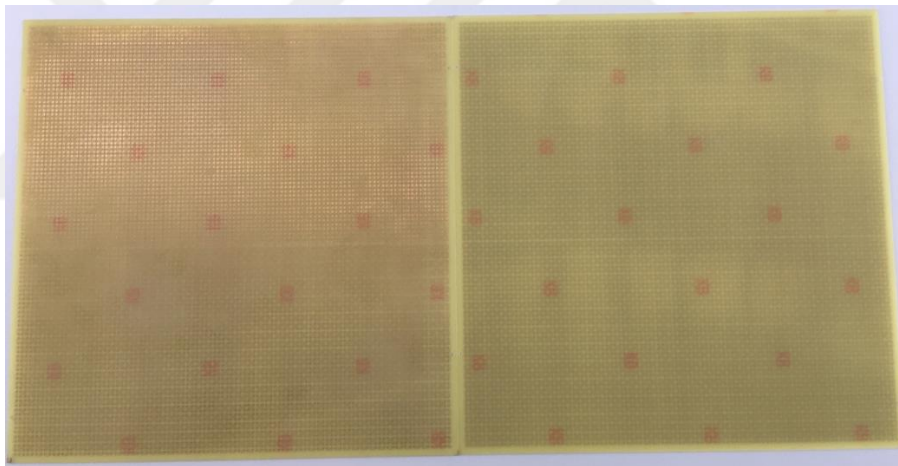


Figure 5. 1 : FSS prototype

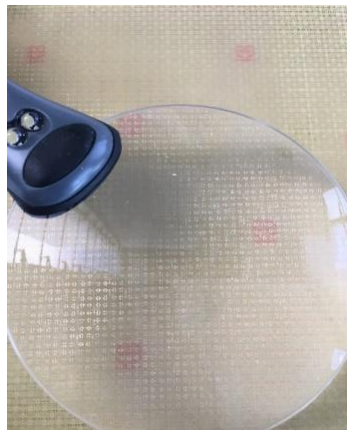


Figure 5. 2 : A close view of the FSS prototype

Support is received from the Profen Group to measure reflection responses of FSS structures. The necessary equipment for the measuring system is provided by this company. In the measurement test, as shown in Figure 5.3, there is a signal generator, signal analyze, Ka band horn antennas and Ku band horn antennas.

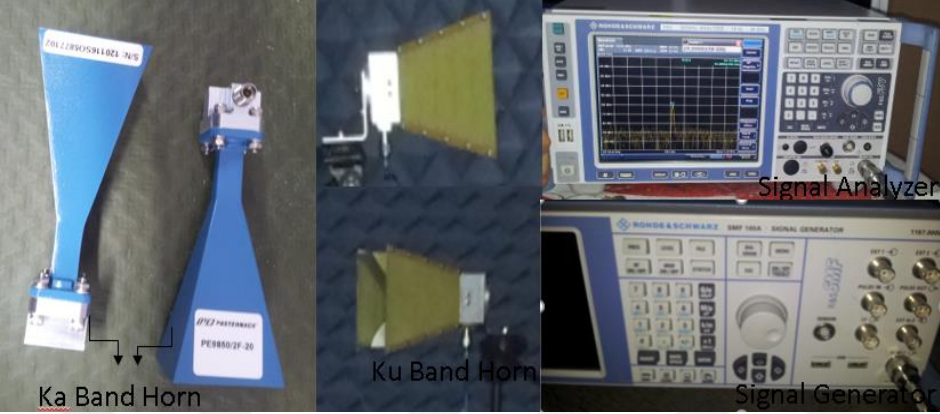


Figure 5. 3 : Measurement Equipment

The test process is carried out in an anechoic chamber to absorb the reflection of electromagnetic waves. Before starting the measurements, empty space measurement is performed without fss to perform the calibration and the results are recorded.

Firstly, the measurement process for Ka band is performed. For this process, the required far-field calculations are made and Ka band horn antennas are placed as far as the calculated amount from FSS. The transmitter antenna is connected to the signal generator and the receiving antenna to the signal analyzer, as shown in Figure 5.4 and Figure 5.5 and the measurement results are taken.

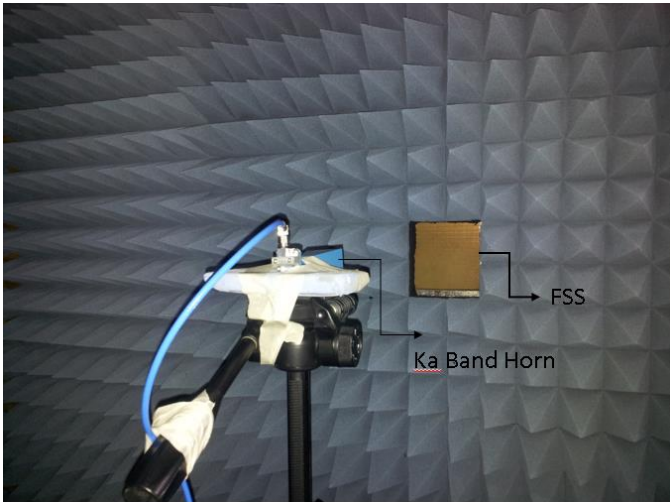


Figure 5. 4 : The location of the FSS in the test setup

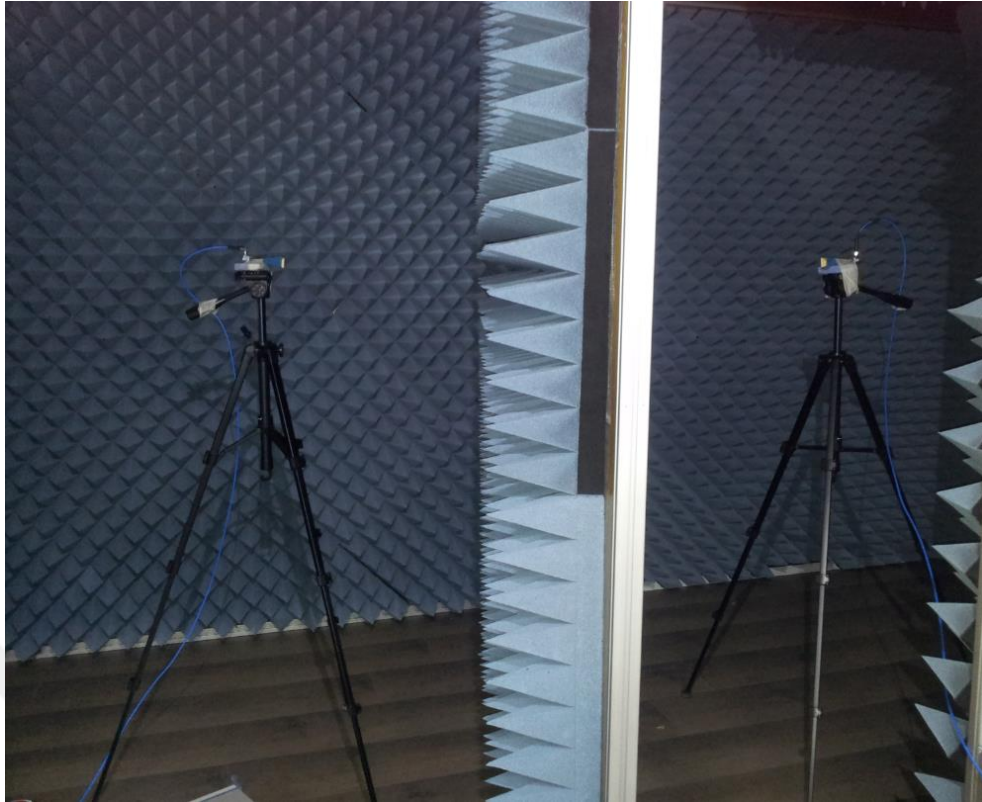


Figure 5.5 : Measurement setup for Ka Band

Secondly, the measurement process for Ku band is performed. For this process, the required far-field calculations are made and Ku band horn antennas are placed as far as the calculated amount from FSS. The transmitter antenna is connected to the signal generator and the receiving antenna to the signal analyzer, as shown in Figure 5.6, Figure 5.7 and the measurement results are taken.



Figure 5.6 : The location of the FSS in the test setup for Ku Band



Figure 5. 7 : Measurement setup for Ku Band

Due to the error in production, the conductive paths could not be printed as desired and therefore the desired values could not be obtained from the measurement. At the same time, it has been decided that the loss of FR-4 layer at high frequencies is very high and is not a good option.

6. CONCLUSIONS AND RECOMMENDATIONS

In this thesis study, three different frequency selective surface have been designed in order to minimize the mass of the satellite, reduce the number of reflectors on the satellite and reduce the cost of the satellite system. The designed structures have been achieved by using Ka, Ku and X band frequencies which are commonly used in satellite applications.

The type of antenna in satellite applications is reflector antenna. Such antennas are consist of three parts: the main reflector, the sub-reflector and the feed. FSSs are used together with reflector antennas in satellite applications, especially as a sub-reflector. The FSS structures models described in section 3.5 are placed as a sub reflector on the reflector antennas. Then the feeds are selected and the signals are sent to FSS. In this work, all of designed FSS have a band stop characteristic; so that the FSS used for the selected bands sends the signals to the main reflective part of the antenna.

In the FSS design with more than one stop band, the geometries in the unit cell determine the stop bands characteristic. Due to the geometries used in design stage, interband interference occurred. Although different geometries were preferred for different frequency bands in the designed FSS, the changed geometric structure for a band also affected the other band. To solve this problem, the distance between geometries designed for different bands is increased and miniaturized structures are used. Analysis results are executed with Ansoft HFSS v.19 software.

In the structure given in detail in Section 4.1, FSS is designed with band stop at different frequencies in Ka band. Proposed hybrid geometry is the combination of two structures on the single layer. Subwavelength geometries are used in the design of a FSS for the desired Ka band. For this structure, a reflection band is observed at 26.5 GHz and 43.5 GHz. Transmission coefficients results are evaluated at different incidence angles for TE an TM polarization. Since the designed structure is not exactly symmetrical, different simulation results are obtained in TE and TM modes.

In the other structure given in detail in Section 4.2, FSS is designed symmetrically. This FSS provides reflection around X band (8 GHz- 12 GHz) and Ka band (38.8 GHz- 41.1 GHz). No interference occurred due to the geometries used in this design. When the structure designed for the Ka band is modified, the X band is not affected by these changes in despite of multiple minimalized structure. So, proposed design has a small element size, dual independent operation band and higher selectivity.

The last FSS structure given in detail in Section 4.3, is capable of reflective electromagnetic waves in Ku band (14.1-16 GHz) and Ka band (29.2 – 36.8 GHz). There are four-arm and two-arm structures placed in different parts of the unit cell in the designed geometry. Interference occurs in this structure because the designed geometries are close to each other and the miniaturized structures are used. In order to prevent both interference and find optimum results at desired frequencies, the equivalent circuit model described in detail in Section 3.3.5.1 is used. For this structure, the transmission coefficient parameters are below -10 dB for both TE and TM polarizations in Ku and Ka band. At the same time, this FSS shows 60 degrees of incidence angle and stable frequency for all polarizations.

In this thesis, FSSs with band stop characteristics are designed at the desired frequency values. The unit cell sizes are reduced in order to achieve the desired frequencies.

Satellite communication technologies are developing quickly. Because of the finitude of frequency bands for satellite communication, they should be used efficiently. Since FSSs are structures capable of changing frequency characteristics, they are important in efficient use of frequency bands. Especially in the defense industry, antenna designs with different radiation patterns and frequencies are used. For this reason, FSSs which can be used in the desired frequency bands are preferred. It is claimed that in this thesis, the frequency selective surfaces which can manage the frequency characteristic according to the needs of the defence industry is designed.

6.1 Improvement of Design Using Different Substrate Layers

The printing and measurement procedures of this design are explained in detail in Chapter 5. As a result of the printing process, it is observed that the structure placed in the middle of the design is printed incorrectly.

To solve this problem, the width (wl) of the structure is increased by 0.05mm. At the same time in order to preserve the size of other structures are enlarged to 1 mm in size. The TE and TM results of the new structure are given in Figure 6.1 and Figure 6.2.

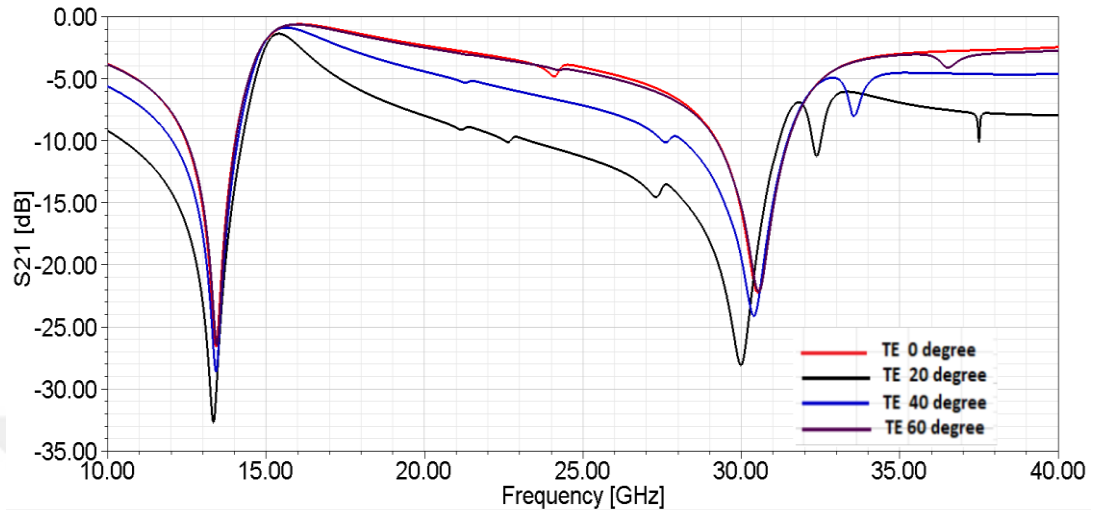


Figure 6. 1 : S_{21} frequency for the fourth FSS geometry,TE polarization

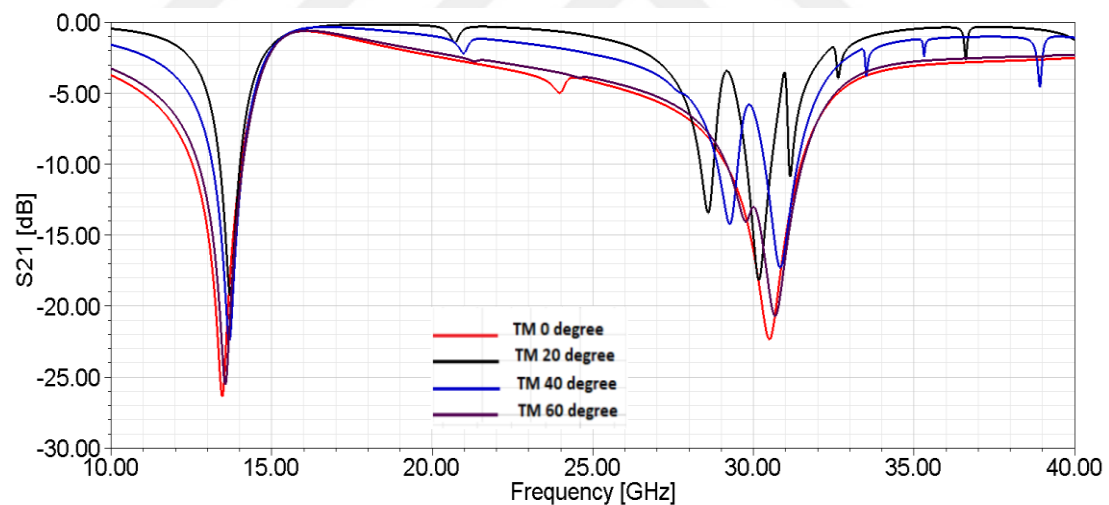


Figure 6. 2 : S_{21} frequency for the fourth FSS geometry, TM polarization

When the design results are examined, approximately 5 GHz shift has occurred in the two frequency bands (Ku and Ka). This change increased the dependence of the design on the angle.

It is decided to use another layer instead of FR-4 to avoid frequency shifting without changing the parameters. At the same time, the loss of this layer at high frequencies is another reason for abandoning this layer.

After the necessary literature review, it is decided to use the Rogers R04350 instead of FR-4 because the loss of this layer at higher frequencies is less. The thickness of the Rogers layer is 1 mm, as in previous designs. At the same time the cell size is 5 mm x 5 mm. The simulation results of this design are given in Figure 6.3 and Figure 6.4.

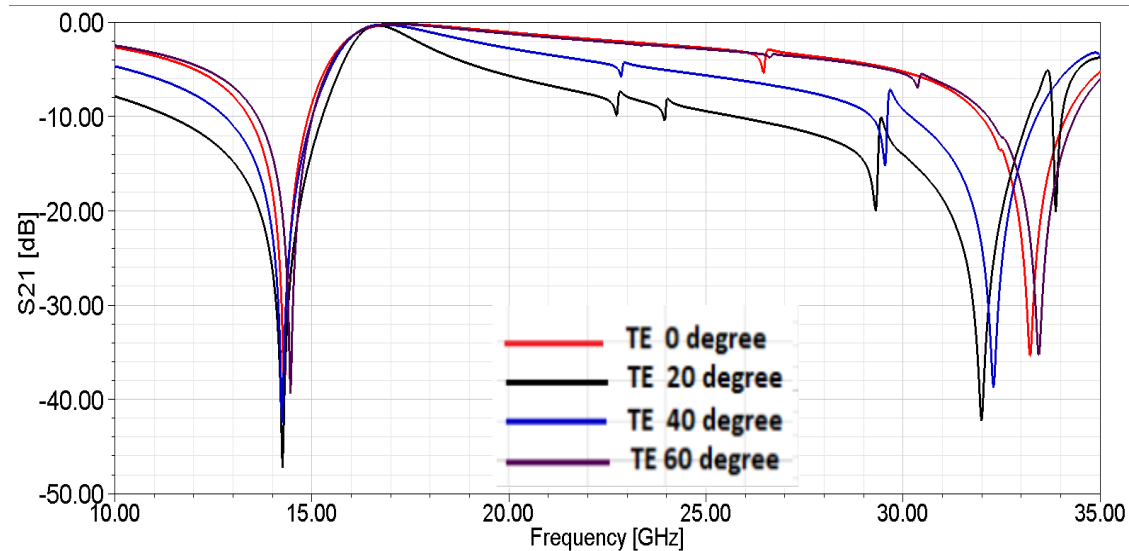


Figure 6. 3 : S_{21} frequency of the FSS designed using Rogers, TE polarization

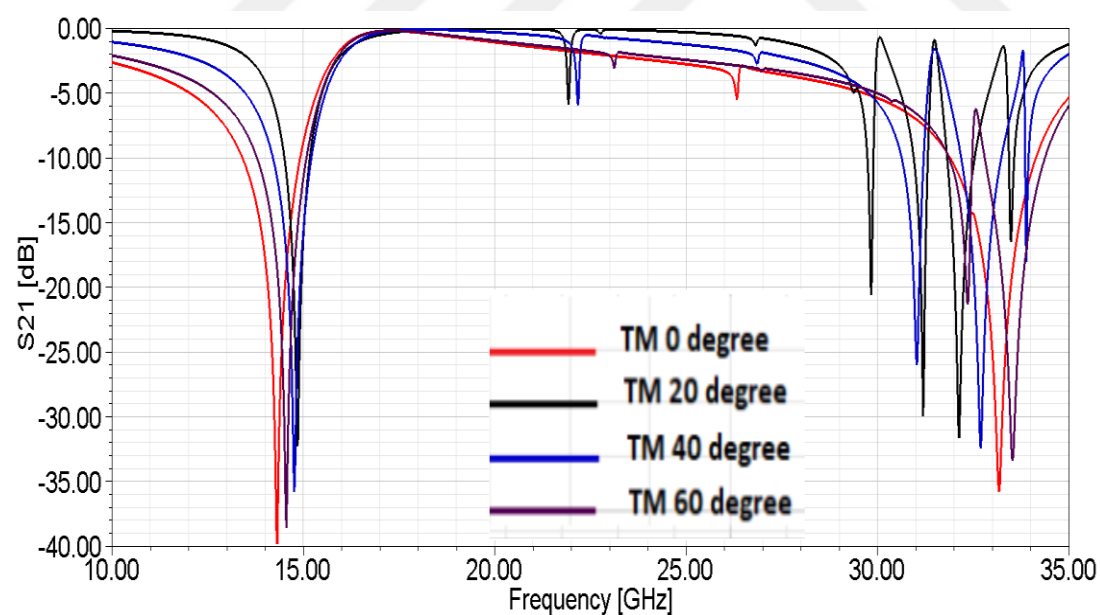


Figure 6. 4 : S_{21} frequency of the FSS designed using Rogers, TM polarization

When the Rogers layer was used, the S_{21} parameter showed a noticeable improvement in both Ku band and Ka band compared to the other designs. According to the simulation results in the fifth design, the transmission coefficient is below -35 dB in both TE polarization and TM polarization.

The reason why this design is not printed is that both the procurement difficulties and the materials are expensive. Due to this situation, it is searched for a material which is easily available and close to the dielectric coefficient Rogers. The dielectric constant of the Rogers layer used in this study is 3.66. Instead of the Rogers layer, it was decided to use Taconic TLC material, which has the closest dielectric constant and is easily available. The dielectric constant of the Taconic TLC material is 3.2. The substrate layer is modified without changing the dimensions of the designed FSS structure. For this structure, TE and TM results are obtained in Figure 6.5 and Figure 6.6.

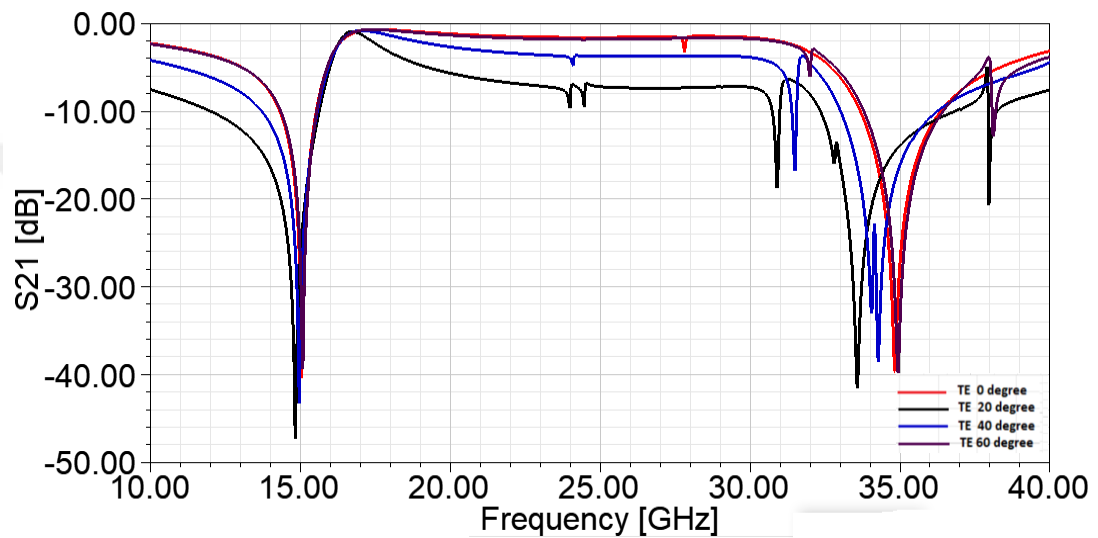


Figure 6. 5 : S_{21} frequency of the FSS using Taconik layer,TE polarization

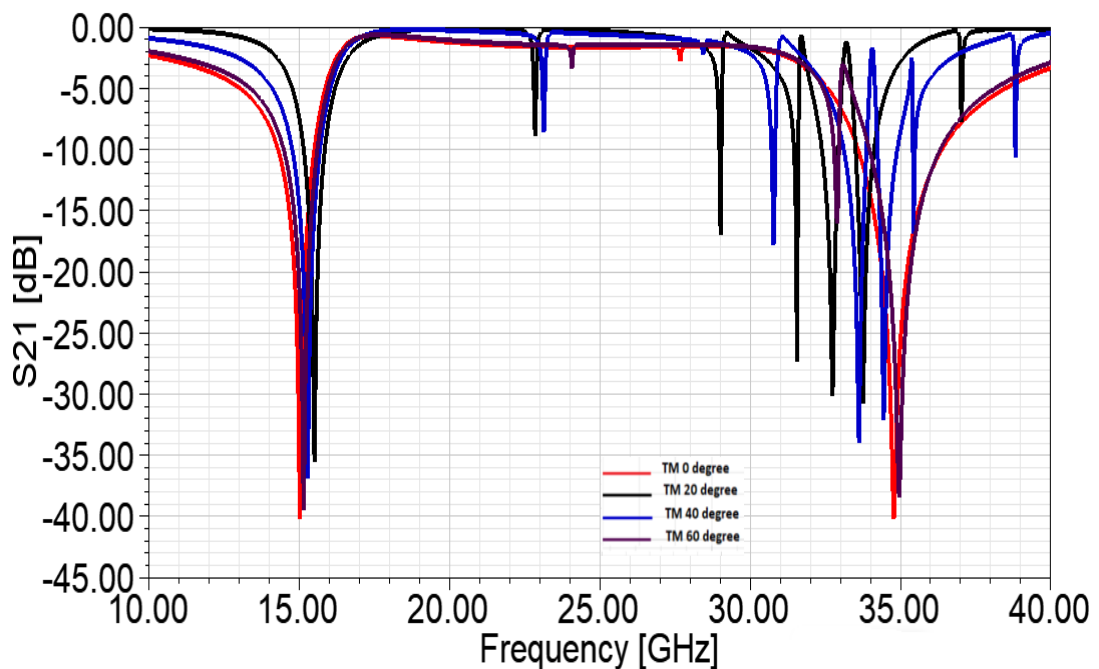


Figure 6. 6 : S_{21} frequency of the FSS using Taconik layer,TM polarization

When the results are evaluated, it is seen that in the TE and TM modes, the resonance frequencies are the same at 0 and 60 degrees. But at 20 and 40 degrees resonance frequencies are shifted. Although this situation increases the dependence on the angle, an approximately -20 dB improvement is observed in the transmission coefficient. The unit cell has been modified to prevent the incidence angle dependence in design. Changes in design are given in Figure 6.7 and TE and TM results are demonstrated in Figure 6.8 and Figure 6.9. When the results are evaluated, it is observed that the shift of resonance occurring at 20-degree and 40-degree incidence angle is decreased.

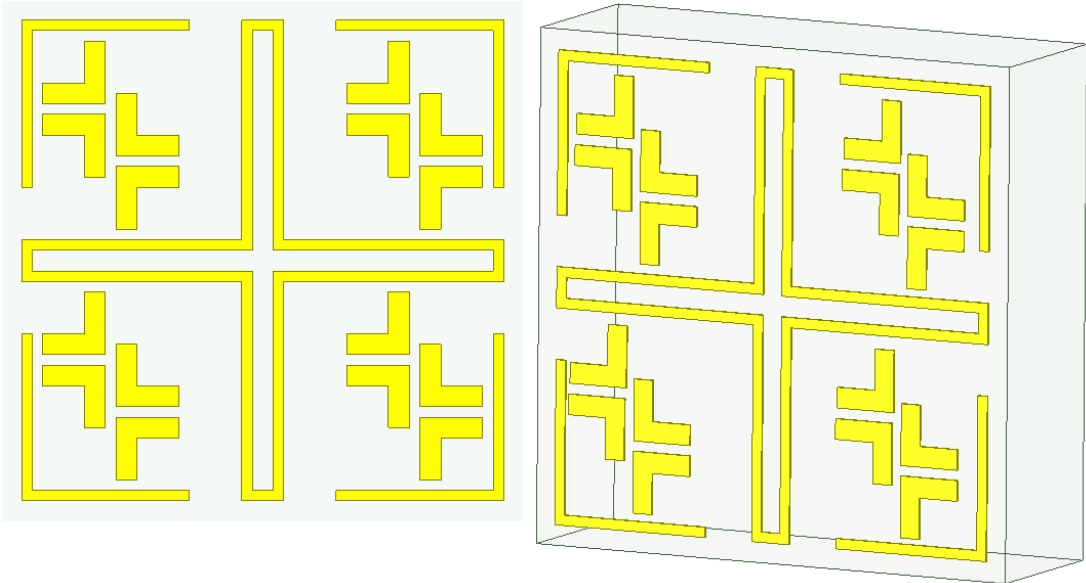


Figure 6. 7 : Modified Design

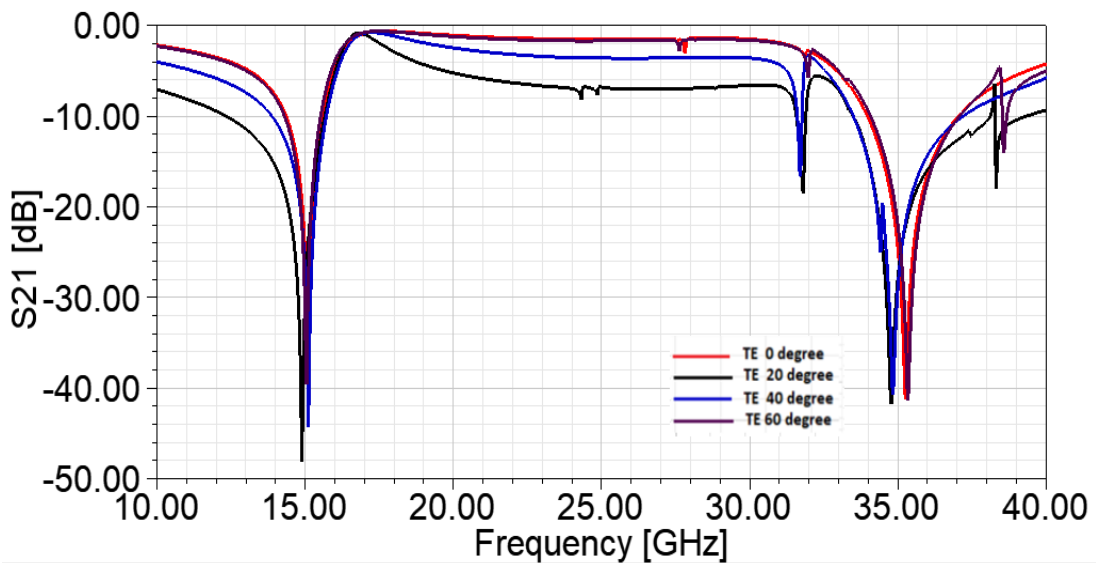


Figure 6. 8 : S_{21} frequency of the new FSS using Taconik layer, TE polarization

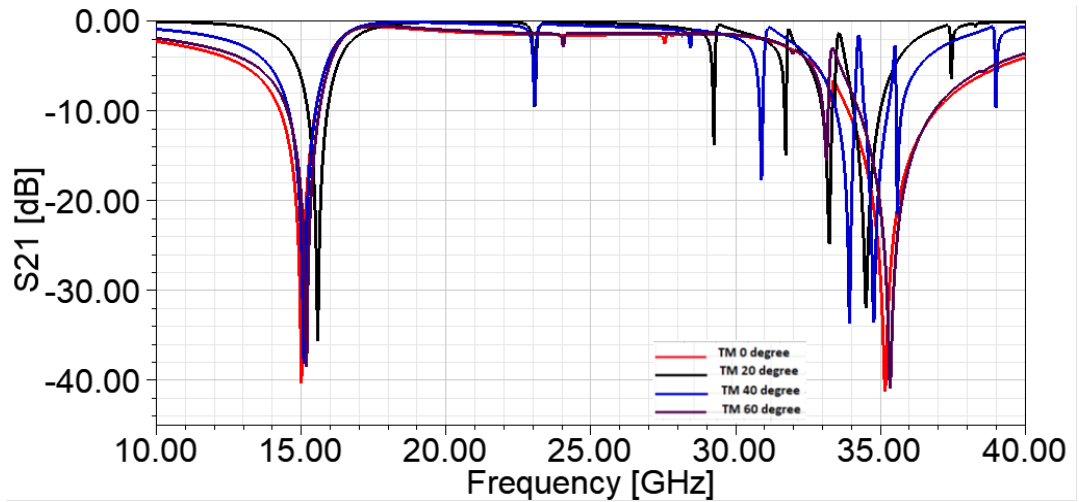


Figure 6. 9 : S_{21} frequency of the new FSS using Taconik layer, TM polarization

The proposed FSS structure in Design 3 was simulated using different substrate layers. The effect of the layer on the resonance frequency was observed. It was seen that there are shifts in the resonance frequency depending on the incidence angle in the layers. In order to reduce the dependence on angle, a few changes were made in the design and the results were evaluated. When the Rogers layers in the literature were examined, it was observed that there were two different models that could be preferred in satellite applications, especially since transmission loss is less. These models are Rogers RO 3003 and Rogers RO 5880. Simulations were repeated using two layers specified without changing the design. Figure 6.10 and Figure 6.11 show the TE and TM polarization results of the FSS designed using the Rogers RO 3003 layer.

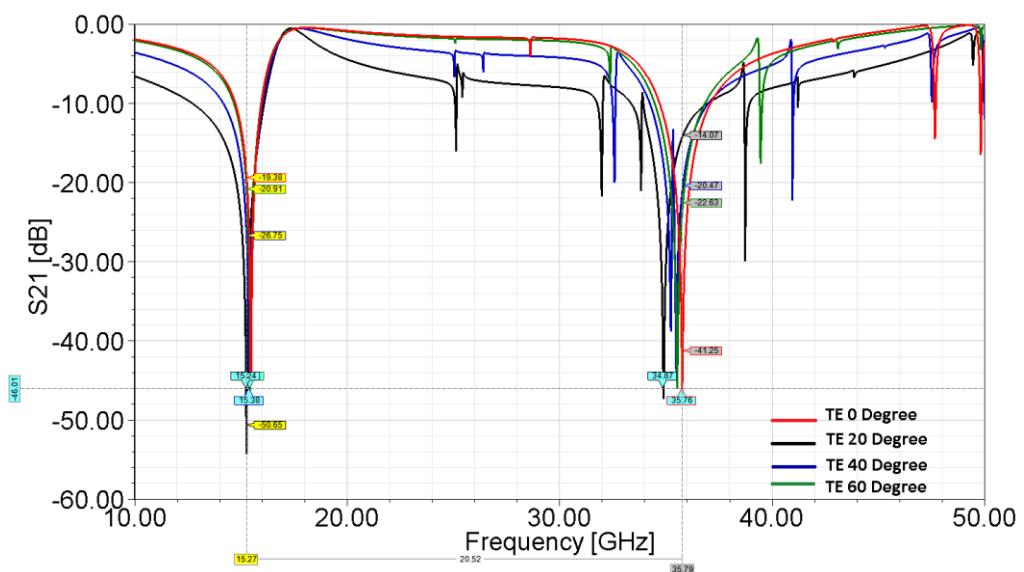


Figure 6. 10 : S_{21} frequency of the FSS using Rogers 3003 layer, TE polarization

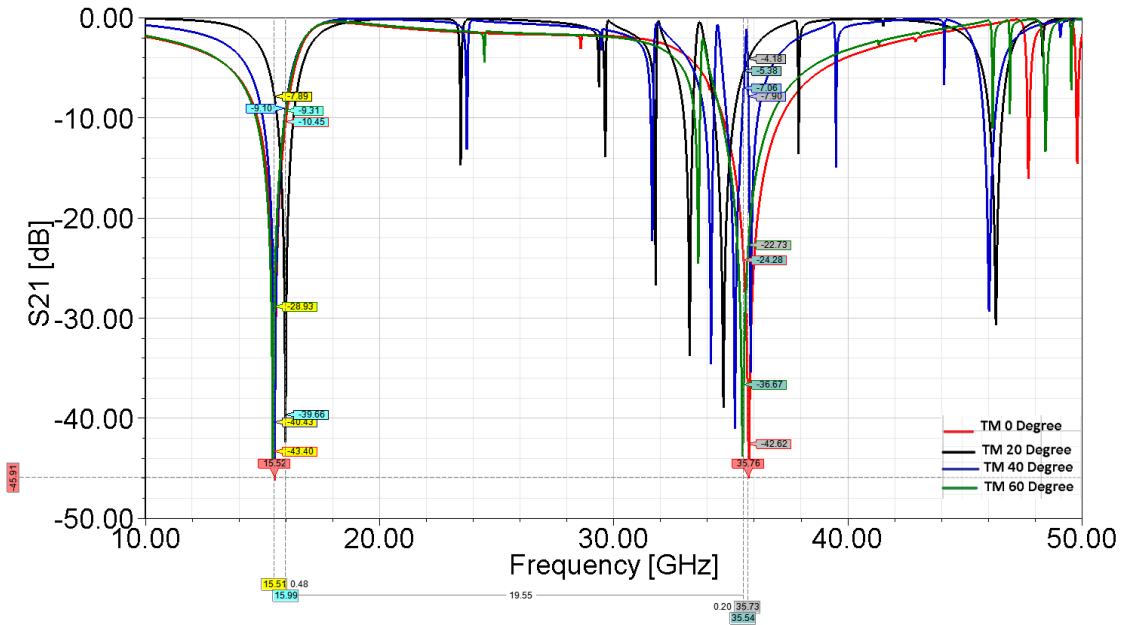


Figure 6.11 : S_{21} frequency of the FSS using Rogers 3003 layer, TM polarization

When the results were examined, it was observed that this layer achieved up to -50 dB in the S_{21} parameter compared to the FR-4 layer and the results were improved. Despite this, it appears to be a dependence to angle. In future studies, this problem can be solved by making some changes in the design. On the other hand, Figure 6.12 and Figure 6.13 show the TE and TM polarization results of the FSS designed using the Rogers 5880 layer.

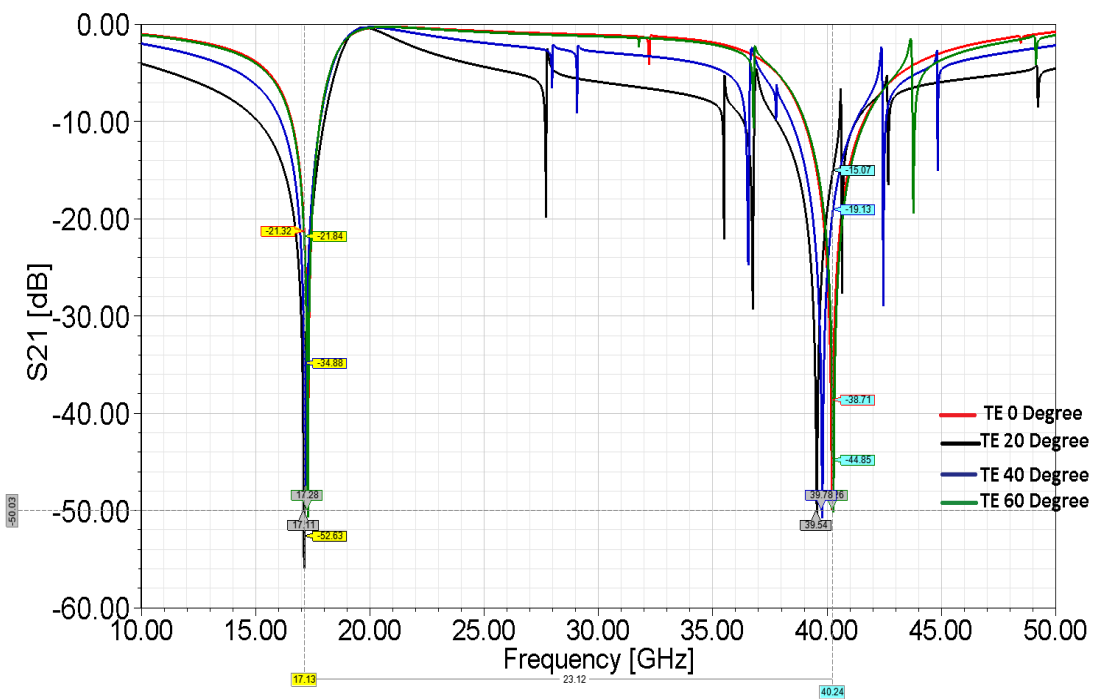


Figure 6.12 : S_{21} frequency of the FSS using Rogers 5880 layer, TE polarization

This layer didn't change the Ku band frequency response compared to Rogers 3003. However, approximately 5 GHz shift occurred at the Ka band center frequency. In future studies, if the thickness of the layer is changed without modifying the design, it is thought that good results will be obtained at the desired frequency.

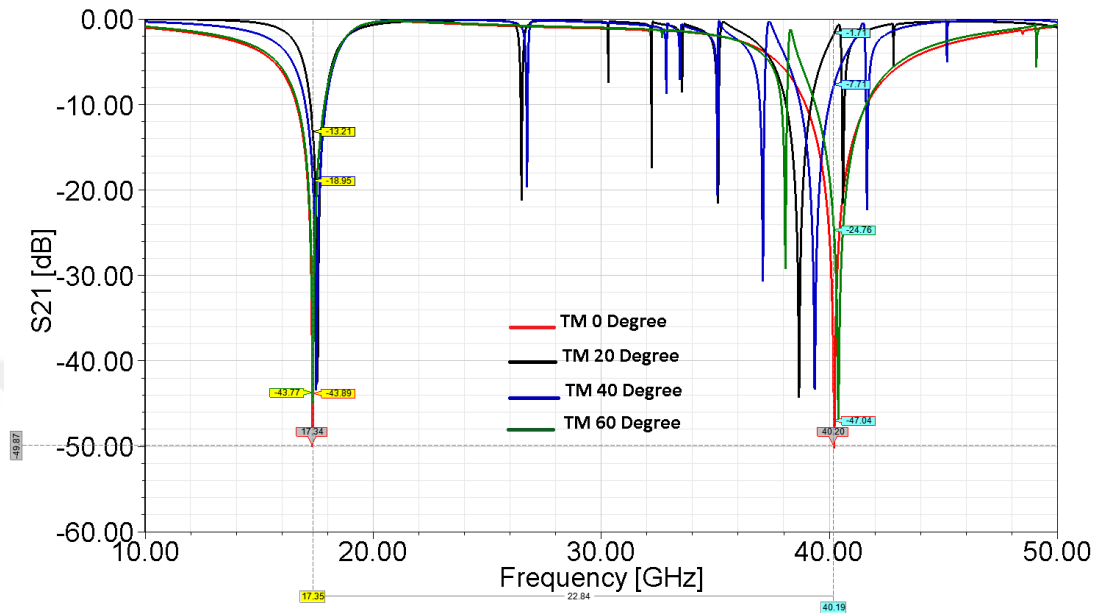


Figure 6. 13 : S₂₁ frequency of the FSS using Rogers 5880 layer, TM polarization



REFERENCES

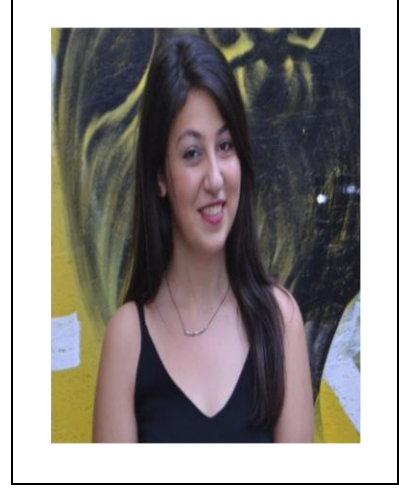
- [1] **Munk, Benedikt A.** (2000). New York Frequency Selective Surfaces: Theory and Design.
- [2] **Chaharmir, Mohammad Reza et al.** (2015). Design of a Multilayer X- / Ka-Band. 63(4): 1255–62.
- [3] **Wu, T.K.** (1995). Frequency Selective Surface and Grid Array. ed. Wiley Interscience Publication.
- [4] **Costa, Filippo, and Agostino Monorchio.** (2012). A Frequency Selective Radome with Wideband Absorbing Properties. *IEEE Transactions on Antennas and Propagation*.
- [5] **Chaharmir, Mohammad Reza et al.** (2015). Design of a Multilayer X-/Ka-Band Frequency-Selective Surface-Backed Reflectarray for Satellite Applications. 63(4): 1255–62.
- [6] **Orr, Robert , Fusco, Vincent et al .** (2015). Circular Polarization Frequency Selective Surface Operating in Ku and Ka Band. *IEEE Transactions on Antennas and Propagation*.
- [7] **Sheng, Xichen, Junxiang Ge, Ke Han, and Xi Cheng Zhu.** (2018). Transmissive/Reflective Frequency Selective Surface for Satellite Applications. *IEEE Antennas and Wireless Propagation Letters*.
- [8] **Zhao, Zhenzhen et al.** (2018). A Novel Dual-Band Frequency Selective Surface with Close Band Spacing at Ka-Band. *IEEE 6th Asia-Pacific Conference on Antennas and Propagation, APCAP 2017 - Proceeding* 1(c): 1–3.
- [9] **Wu, Weiwei, Liu, Xiuhan, Cui, Kaibo et al** (2018). An Ultrathin and Polarization-Insensitive Frequency Selective Surface at Ka-Band. *IEEE Antennas and Wireless Propagation Letters* 17(1): 74–77.
- [10] **Al-Joumayly, Mudar, and Nader Behdad.** (2009). A New Technique for Design of Low-Profile, Second-Order, Bandpass Frequency Selective Surfaces. *IEEE Transactions on Antennas and Propagation*.
- [11] **Salehi, Mohsen, and Nader Behdad.** (2008). A Second-Order Dual X-/Ka-Band Frequency Selective Surface. *IEEE Microwave and Wireless Components Letters* 18(12): 785–87.
- [12] **Sarabandi, Kamal, and Nader Behdad.** (2007). A Frequency Selective Surface with Miniaturized Elements. *IEEE Transactions on Antennas and Propagation*.
- [13] **Barry, Evans.** (2008). *Satellite Communication Systems*. Institution of Engineering and Technology.

- [14] **Pelton, Joseph N., Scott Madry, and Sergio Camacho-Lara.** (2013). Handbook of Satellite Applications Handbook of Satellite Applications.
- [15] **Wheeler, Harold A.** (1947). A Helical Antenna for Circular Polarization. Proceedings of the IRE.
- [16] **Haddad, Mohammed T Al.** (2016). Design of Frequency Selective Surface (FSS) for Mobile Signal Shielding By.
- [17] **Döken, Bora.** (2014). Amaca Uygun Olarak Yansıma ve İletme Karakteristikleri Değişebilen Yüzey Malzemesi Tasarım. Istanbul Technical University.
- [18] **Skinner, Neal G, and Dale M Byrne.** (2006). Finite-Difference Time-Domain Analysis of Frequency-Selective Surfaces in the Mid-Infrared. 45(9): 1943–50.
- [19] **Davidson, D B, A G Smith, and J J Van Tonder.** (1997). The Analysis, Measurement and Design of Frequency Selective Sur- Faces. (436): 14–17.
- [20] **Bardi, Istvan, Richard Remski, David Perry, and Zoltan Cendes.** (2002). Plane Wave Scattering from Frequency-Selective Surfaces by the Finite-Element Method. In IEEE Transactions on Magnetics.
- [21] **Lou, Hung.** (2006). Modal Analysis and Design of Compound Gratings and Frequency Selective Surfaces. University of Colorado.
- [22] **Mitra, Raj, Chi H. Chan, and Tom Cwik.** (1988). Techniques for Analyzing Frequency Selective Surfaces-a Review. Proceedings of the IEEE.
- [23] **GH, Dadashzadeh, Amini AR, and Mallahzadeh MH.** (2014). Equivalent Circuit Model for Square Ring Slot Frequency Selective Surface. Journal Of Communication Engineering.
- [24] **Nathan Marcuvitz.** (1986). Waveguide Handbook. Stevenage, UK: Institution of Electrical Engineers.
- [25] **Campos, Antonio L.P.S., Adaildo G. D’Assunção, Robson H.C. Maniçoba, and Lincoln M. Araújo.** (2012). Software for Project and Analysis of Frequency Selective Surfaces. Journal of Microwaves, Optoelectronics and Electromagnetic Applications.
- [26] **Yilmaz, Asim Egemen, and Mustafa Kuzuoglu.** (2009). Design of the Square Loop Frequency Selective Surfaces with Particle Swarm Optimization via the Equivalent Circuit Model. Radioengineering.
- [27] **Parker, EA.** (1991). The Gentleman’s Guide to Frequency Selective Surfaces. *17th QMW Antenna Symposium (April):* 1–18. http://www.eda.kent.ac.uk/material/pdf_docs/FSS_Guide.pdf.
- [28] **Costa, Filippo, Agostino Monorchio, and Giuliano Manara.** (2014). An Overview of Equivalent Circuit Modeling Techniques of Frequency Selective Surfaces and Metasurfaces. Applied Computational Electromagnetics Society Journal.

- [29] **Sung, Grace Hui Hsia, Kevin W. Sowerby, Michael J. Neve, and Allan G. Williamson.** (2006). A Frequency-Selective Wall for Interference Reduction in Wireless Indoor Environments. *IEEE Antennas and Propagation Magazine*.
- [30] **Jenn, David C.** (2005). *Springs Radar and Laser Cross Section Engineering*.
- [31] **Agrawal, Vishwani D., and William A. Imbriale.** (1979). Design of a Dichroic Cassegrain Subreflector. *IEEE Transactions on Antennas and Propagation*.
- [32] **Wu, Te Kao.** (1994). Four-Band Frequency Selective Surface with Double-Square-Loop Patch Elements. *IEEE Transactions on Antennas and Propagation*.
- [33] **Comtesse, L. E., R. J. Langley, E. A. Parker, and J. C. Vardaxoglou.** (1987). Frequency Selective Surfaces in Dual and Triple Band Offset Reflector Antennas. *In 17th European Microwave Conference*.
- [34] **Bayatpur, Farhad.** (2009). *Metamaterial-Inspired Frequency-Selective Surfaces*. Tese de doutorado.
- [35] **Gao, Meng, Seyed Mohamad, Amin Momeni, and Hasan Abadi.** (2016). A Dual-Band , Inductively Coupled Miniaturized-Element Frequency Selective Surface With Higher Order Bandpass Response. *IEEE Transactions on Antennas and Propagation*.
- [36] **Liu, Ning, Xianjun Sheng, Chunbo Zhang, and Dongming Guo.** (2018). Design of Frequency Selective Surface Structure with High Angular Stability for Radome Application. *IEEE Antennas and Wireless Propagation Letters*.
- [37] **Mohamad, Seyed et al.** (2015). Inductively-Coupled Miniaturized-Element Frequency Selective Surfaces With Narrowband, High-Order Bandpass Responses. *63(11): 4766–74*.



CURRICULUM VITAE



Name Surname: Esmat Mutluer

Place and Date of Birth: Nazilli, 17.11.1991

Address: Mecidiyeköy, İstanbul

E-Mail: esmamutluer91@gmail.com

B.Sc.: Pamukkale University – Electrical Electronics Engineer

Professional Experience and Rewards:

System Specialist, ITU Research and Application Center for Satellite Communication and Remote Sensing, **İstanbul-Turkey**, January 2018– Currently.

Student Researcher, ITU Research and Application Center for Satellite Communication and Remote Sensing, **İstanbul-Turkey**, September 2017 – January 2018.

PUBLICATIONS/PRESENTATIONS ON THE THESIS

- **Mutluer E.**, Döken B., Kartal M., 2018, A Novel Multi-Band Frequency Selective Surface for Ka-Band Applications , *the Seventh International Conference on Telecommunications and Remote Sensing*, October 8–9, Barcelona, Spain.
- **Mutluer E.**, Döken B., Kartal M., 2018, A Miniaturized Dual Ka/X Band Frequency Selective Surface, *3rd International Mediterranean Science and Engineering Congress*, October 24-26, Adana, Turkey.
- **Mutluer E.**, Döken B., Kartal M., 2018, A Dual-Band Frequency Selective Surface Design for Satellite Applications, *The 18th Mediterranean Microwave Symposium*, 31 October-2 November, İstanbul, Turkey.